ELSEVIER

Check for updates

Microneedle technology as a new standpoint in agriculture: Treatment and sensing

Emre Ece [a], Ismail Eş [a,*], Fatih Inci [a,b,*]

[a] UNAM-National Nanotechnology Research Center, Bilkent University, 06800 Ankara, Turkey
[b] Institute of Materials Science and Nanotechnology, Bilkent University, 06800 Ankara, Turkey

Preventing plant loss and improving their health status are essential for agricultural industry. Correspondingly, the deprivation of plants severely impacts our ecological system. As such, global efforts have been intensely made to promote the development of advanced sensing and treatment platforms to forestall plant loss. Existing technologies mainly encounter a number of challenges in providing results in a non-invasive, rapid turnaround, and affordable fashions. Accordingly, notable progressions in innovative approaches—particularly biosensing and delivery platforms, are vastly required for agriculture realm. In this regard, microneedles have emerged as a pivotal technological tool that plays multifaceted roles in biosensing and delivery systems, with attention of growing towards agriculture. Simply put, microneedles offer several advantages over conventional methods for being less invasive, rapid, and highly precise. In this review, recent advancements in microneedle technologies including their implementations in agriculture are highlighted coherently. In particular, extracting DNA from plant leaves and expressing transient genes using microneedles are elaborated in details. Microneedle-based sensing platforms for detecting essential compounds and secondary metabolites are discussed as well. Recent advances focusing the delivery of agrochemicals and nanotherapeutics via microneedles are elaborated. By this means, this review aims to bridge the existing gaps between microneedles and agriculture precisely.

Keywords: Agricultural products; Crop diseases; Microneedles; Biosensors; Drug delivery

Introduction

The global population is estimated to be 8.5 billion people in 2030, reaching 9.7 and 10.9 billion by 2050 and 2100, respectively [1]. This implies a growing demand for agricultural products, the most valuable commodities to manufacture a great variety of food constituents [2]. Concerns regarding the safety and quality of crop products have exceptionally increased, compelling global regulatory agencies such as Food and Agriculture Organization (FAO) and Food and Drug Administration (FDA) to urgently introduce strict regulations for guiding stockholders and farmers to assure the safety of the agricultural products [3]. Despite these robust directions, agricultural products have been perpetually confronted by diseases and contaminants, causing a significant drop in crop yield and eliciting safety issues for consumers [4]. That being said, plants are either treated with pharmaceutical compounds to boost their health status against external factors or exposed to a high dose of agrochemicals to prevent crop loss [5].

The excessive use of agrochemicals typically results in accumulating potentially hazardous compounds in trace amounts in crops, adversely striking the measures taken during post-harvest processes (i.e., packing, storing, and transporting) [6]. To address this issue, agrochemicals are utilized within the recommended limits of the *Codex Alimentarius* set by FAO and the

* Corresponding authors at: UNAM-National Nanotechnology Research Center, Bilkent University, 06800 Ankara, Turkey.
E-mail addresses: Eş, I. (ismail@unam.bilkent.edu.tr), Inci, F. (finci@bilkent.edu.tr).

1369-7021/© 2023 Elsevier Ltd. All rights reserved. https://doi.org/10.1016/j.mattod.2023.07.002

World Health Organization (WHO) [7]. Therefore, agricultural products are thoroughly tested in laboratories using detection techniques to ensure that they meet the quality and safety standards and comply with regulatory limits for contaminants [8]. Analytical chemistry has made considerable progress in past decades, granting the detection of contaminants in agricultural products at trace amounts [9]. Despite the establishment of a diverse number of techniques for rapid and sensitive screening, the complexity in the screening of such compounds remains since the limits permitted by *Codex Alimentarius* for specific agrochemicals are exceedingly low, and the life-threatening effects of agrochemicals on public health and the environment are factual. Existing technologies mainly encounter a number of challenges in providing results in a non-invasive, rapid turnaround, and affordable manner. On account of this technical complication, new techniques enabling rapid and precise monitoring of analytes, preferentially in a single run, are required. Besides, the on-field delivery of agrochemicals or agri-pharmaceuticals to the crops with current techniques (e.g. dusting and spraying) is highly invasive and laborious [10]. Hence, constructing innovative strategies and modalities would promote precise delivery of these chemicals, significantly reducing residual pollution; thereby creating a more sustainable agricultural system and annihilating concerns regarding food safety [11]. Accordingly, notable progressions in innovative approaches both for biosensing and delivery systems have been made for agriculture realm.

On the other hand, analyzing agrochemicals is performed briefly by taking tissue samples from xylem and phloem of the plants. On the course of the sampling process, plants often fail to survive the invasion of a thick probe, which leads to the emergence of a non-invasive technology to be exploited [12]. In this regard, microneedles (MNs) have emerged as a major technological tool that plays a plethora of roles in delivery and biosensing systems, with an attention of growing towards agriculture. Typically, MN platform consists of micron-sized arrays that are systematically arranged on a miniature patch. MN arrays can be fabricated in different geometries (e.g., pyramid and conical) [13] with a length and width of 25–2000 μm and 50–250 μm, respectively [14,15]. MNs, depending on their classification, can be also fabricated by employing diverse methods such as 3D printing [16], dry & wet etching processes [17], micro milling [18], and laser ablation [19].

MNs can be classified into four sub-categories where each MN type plays a different role in agricultural application. Solid MNs are the basic form of MNs and can be employed to pre-treat the surface of plant tissue for facilitating further administration of agrochemicals,[20] while hollow MNs consist of a reservoir to separately introduce agri-pharmaceuticals through the hollow structures [21]. Coated MNs are usually a type of solid MN with their tips covered with specific biomolecules to capture biomarkers [22]. Finally, dissolving MNs are made of water-soluble materials and release the drugs upon penetration through the skin of plants/animals [23]. Simply put, MNs offer several advantages over conventional methods for being rapid, less invasive, and highly precise. Considering these fashions, novel nanotherapeutics have been effectively delivered to the stem tissues of infected trees [22]. MNs have been integrated with a nucleic acid amplification platform for rapid detection of plant diseases and screening plant pathogens [24]. Continuous monitoring of key physiological features of plants such as the level of polyphenolics [25], water transportation status [26], abscisic acid levels [27], salicylic acid and pH levels [28], and different ion species [29] is also among the application of MNs in agriculture.

The use of MNs as a biosensing and delivery system in agricultural products is still in its infancy and available literature on this topic is limited [30]. There is an urgent demand for more reliable MN-based delivery and detection systems to provide early feedback to farmers and food control agencies. Overall, the design parameters of MNs need to be further investigated for developing a more accurate delivery and detection tool for agriculture. To the best of our knowledge, existing literature mainly focuses on using MNs in animals and artificial skins from drug delivery and sampling perspectives in diseases. There is also a growing interest in using MNs for agricultural purposes. As an example, a review of the current research on MNs in agriculture is timely in assessing the potential benefits and limitations of this technology. In our review, we expansively explore global agricultural industry under the shadow of crop diseases and identify main technological weakness of current methods in sensing and treatment. Following this, we point out the significance of MNs as a promising alternative and integrative tool to the current agrotechnologies, providing a new perspective to agricultural detection and treatment studies (Fig. 1). Conclusively, we aim to bridge the existing gaps between MNs and agriculture precisely to provide valuable insight into this promising area of research with significant potential for improving the sustainability and efficiency of agriculture.

Global agricultural industry under the shadow of crop diseases

Agriculture has been effectuating ecological and economic sustainability since 10,000 BCE [31,32]. Due to the increasing world population and demand for food products, investment in the agriculture industry becomes essential expeditiously. Wheat, maize, soybeans, rice, oil palm, barley, bananas, and rapeseed are among the top agricultural commodities in global export quantity [33]. According to the global report of FAO, wheat is the most exported agricultural product, with a 198 million tons value in 2020 (Fig. 2**a**) [33]. On the other hand, soybean has the most economical export value, with US$ 64 billion in 2020 [34]. Regrettably, tones of agricultural products have been lost due to plant diseases, which adversely impact the global economy [35]. These diseases have an immense impact on global economy (Fig. 2**c**). For instance, FAO has reported that plant diseases cost the global economy over $220 billion each year [36]. As a result of enormous harm caused by plant disease and contaminants, technological advancement in detection and treatment is essential to curb or minimize the effects of these diseases.

Currently available techniques for diagnosis and screening of agricultural products rely on separation, purification, and detection processes using chromatographic, spectrophotometric, and analytical tools, whereas conventional bulk sprayers are employed for prevention and treatment processes [37–41]. Various detection techniques have been developed for use in agriculture, but they are often invasive, requiring a large area and the

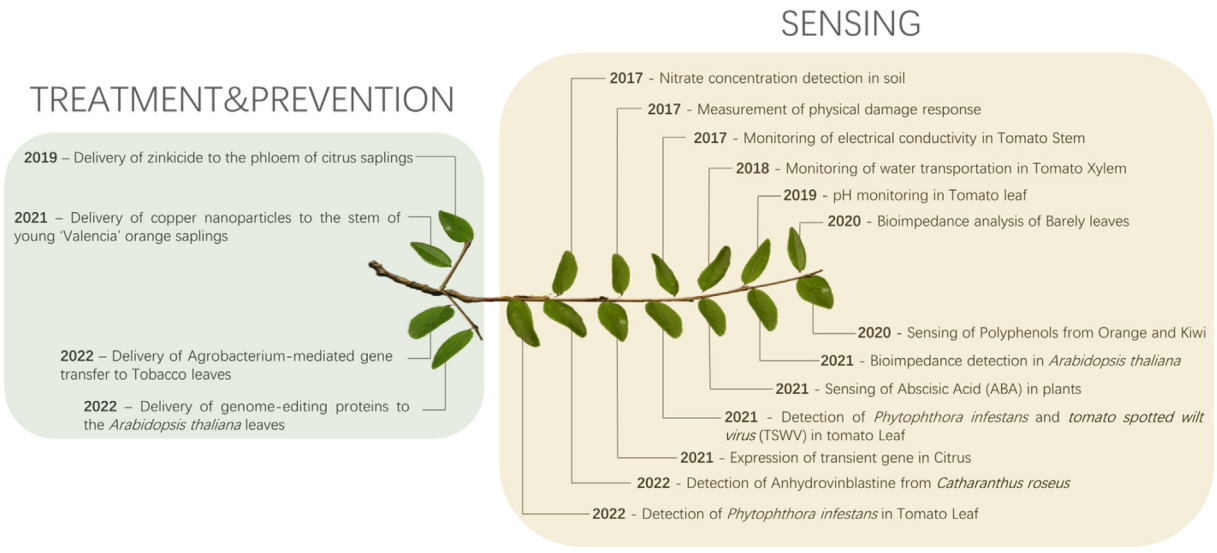

FIG. 1

Timeline shows the application of microneedles in agricultural products for treatment & prevention (left) [18,22,182,188] and sensing purpose (right) [24–27,29,143,156,164,167,168].

use of hazardous chemicals for sample preparation [24]. Furthermore, they are expensive and require qualified personnel [42]. Therefore, there is a need for more portable and user-friendly tools that can be easily transported and accessible worldwide, particularly for in-field applications [43]. These tools should also be affordable, environmentally friendly, and suitable for universal and in-field use.

Effective treatment and prevention methods are necessary to ensure food safety, improve crop yield and quality, protect the environment, and promote economic growth in the agricultural industry. Pesticides, soil enrichment processes, and genetic materials have been used to treat crop diseases and improve crop health [44–47]. However, these treatment techniques have drawbacks, such as the excessive use of hazardous agrochemicals, which can accumulate in the soil and crops at trace levels, posing risks to the ecosystem. More efficient and environmentally friendly approaches should be developed and implemented to eliminate these risks. Various delivery methods, such as dusting, spraying, and seedling root dip, have been developed for pesticide application [48]. In addition, more advanced techniques such as CRISPR-Cas have been employed to engineer plant genomes for disease prevention and increased crop yield.

Microfluidic systems [49], sensors [50–56], and paper-based flexible materials [57] are commonly used in biomedicine and biotechnology and have been adapted as point-of-care tools for plant disease detection. Lab-on-a-chip devices [58,59], loop-mediated isothermal amplification (LAMP) systems [60], and direct tissue blot immunoassays (DTBIA) [61] are among the

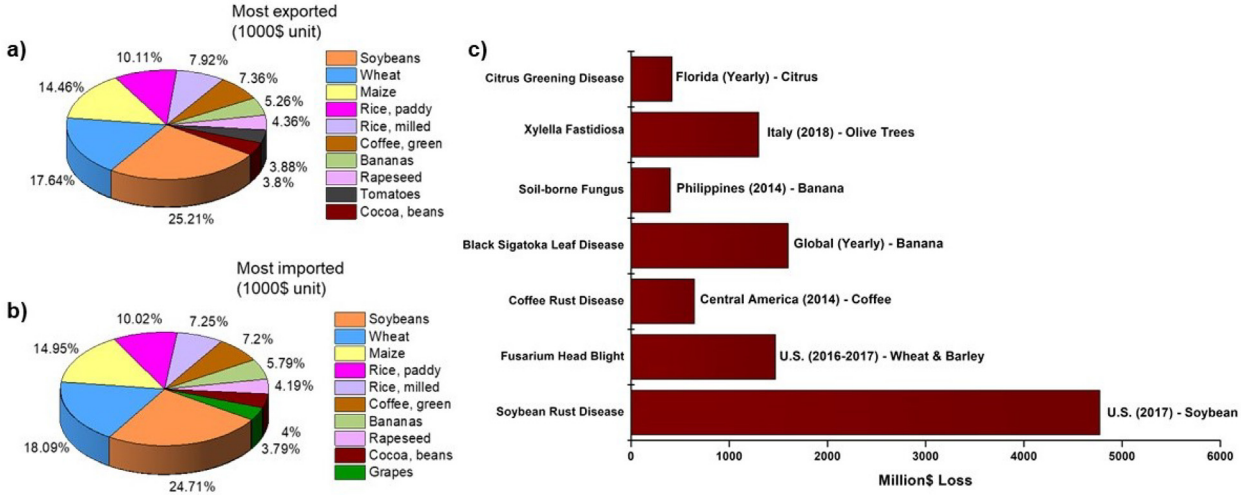

FIG. 2

Global trade values of top 10 agricultural products in 2020 and the crucial plant diseases with economic burdens were summarized. (a) Top 10 exported and (b) imported products were presented. The processed crops and livestock products were excluded in the list. The graphics (a,b) were prepared according to the Food and Agriculture Organization Corporate Statistical Database [33]. (c) Crop diseases, including citrus greening disease [206], Xylella fastidiosa [207] (accessed date: 10/04/23), soil-borne fungus [208], black sigatoka leaf disease [209], coffee rust disease [210], fusarium head blight [211], and soybean rust disease [212], and their economic burdens in USD million were listed.

technologies used to detect plant diseases. These tools have significantly reduced the cost of detection compared to conventional methods such as ICP-MS and AAS mass spectroscopy, and they allow for the determination of highly infectious pathogens in small sample volumes, providing an opportunity for immediate crop treatment and prevention of further contamination.

An innovative approach that we focus here, MN technology, is being used to minimize the damage given to plants during sampling or analysis, making it a milestone approach in agriculture [62]. MNs can be applied directly to plants without interfering with their metabolism and can also be used to release essential molecules such as agrochemicals, nucleic acids, and minerals. This technology can also lessen the harmful effects of pesticides on the environment. Innovative technologies such as patch-on-a-chip, lab-on-a-chip, and next-generation biosensors would gain more beneficial use with the integration of MNs [63–65].

Current microneedle technology for agricultural realm

The concept of MNs was first proposed in 1976 [66]; however, it was not introduced experimentally as an alternative tool in transdermal drug delivery until the late 1990 s due to the limitations encountered in microfabrication techniques [67]. MNs are micron-sized needles, ranging from 25 to 2000 μm in height, constructed in various shapes (e.g., conical and pyramidal) utilizing a wide range of materials and fabrication methods [15,68]. Although most of the investigations have mainly focused on animals, subsequent research in MN fabrication in recent years has accelerated their implementation into different fields, notably in agriculture. Unlike traditional methods, MNs' minimally invasive fashion offers a crucial advantage over traditional methods by minimizing plant health damage upon insertion [26] and providing reusability for in situ applications, especially on farms [69].

In recent years, the agriculture industry has begun using MNs to treat plant diseases, monitor plant health, and detect agrochemicals and pathogens. However, current tools for treatment, prevention, and biosensing in agriculture are often invasive and ineffective, relying on agrochemicals or inefficient biomarker capture [70–72]. To achieve a more effective, precise, and rapid outcome, MNs have been progressively modified in terms of type, material, and geometry. The architecture of MNs, including their height, base diameter, aspect ratio, the radius of curvature, and tip angle is vital in MN design and determines how MNs interact with target tissues (Fig. 3) [73]. For instance, MNs with higher aspect ratio can penetrate into cuticle — plant skin that covers the above-ground surfaces — reaching the deeper layers. The shape of MNs can also affect their ability to penetrate the skin. Shorter MNs may not penetrate as deeply while longer MNs will reach the deeper skin layer. Spacing between each MN array will have a different impact on the delivery of therapeutic agents. If the spacing between MN arrays is extensive, MNs may not be able to sample enough fluid from plants to accurately detect the target analyte. MNs' ability to penetrate plant tissue is crucial for creating pathways that facilitate the transport of macromolecules [74]. To enhance penetration in specific plant regions, researchers adjust the aforementioned features using various fabrication techniques [75].

These attributes must be designed and fabricated based on the thickness of plant parts to be treated. For instance, the midrib of a mature four-week-old *Arabidopsis thaliana* has a thickness ranging from 260 to 366 μm [76]. MNs' surface characteristics and the plant's mechanical features are crucial in their interactions with plant tissue, especially when used for delivery or biosensing. Roughness can hinder the MN-plant tissue interaction, affecting adsorption and release kinetics [77]. The release kinetics of MNs refer to how the active substance (drug or analyte) is either released or captured over time. For example, zero-order release kinetics includes the transport of macromolecules at a constant rate over time, regardless of its concentration, whereas in the first-order kinetics, target molecule is transported from MNs to the tissue or vice versa at a rate that is proportional to the concentration [78]. MNs can be also programmed to possess burst release kinetics, in which active substance is rapidly transported in a short period of time, followed by a slower as well as sustained release over a longer period [79]. Overall, the fabrication method and material selection, as well as design parameters [79–81], erratically affect the outcome of treatment and detection processes [82]. This section will further discuss MN types, fabrication methods and materials used in their design mainly considering applications directed toward agricultural products.

Microneedle types

MNs can be classified as solid, coated, dissolving, and hollow (Fig. 3) [14]. They greatly differ from each other with regard to the application mechanism (delivery or biosensing), fabrication method (Fig. 4), and materials used in their design. Solid, coated, dissolving, and hollow MNs operate in “poke-and-patch”, “coat-and-poke”, “poke-and-release”, and “poke-and-flow” mechanisms, respectively. Here, we will briefly introduce each MN type, covering their potential relevance in agricultural applications.

Solid microneedles

Solid MNs are used to pre-treat plant tissues for the delivery of agrochemicals [18]. This two-step process, known as “poke-and-patch,” involves applying MNs to the plant tissue to create temporary micropores on the surface, which allows for more effective exposure to agrochemicals (Fig. 3**a**) [83]. The design of solid MNs varies depending on the desired geometric features, with higher aspect ratios and lower tip angles requiring more sophisticated techniques and advanced materials [84].

Solid MNs’ composition affects their mechanical strength, biocompatibility, and reusability. Silicon is commonly used for solid MN fabrication due to its superior biocompatibility and mechanical strength compared to other materials [85]. Besides silicon, metals such as titanium (Ti) [86], Tungsten (W) [87], and stainless steel [88] as well as polymers such as poly (methyl vinyl ether) (PMVE) [89], poly(methyl methacrylate) (PMMA) [90] are extensively used as the main component in solid MNs fabrication [91–93]. Furthermore, biocompatible materials such as poly(lactic acid) (PLA) [94] and chitosan [95] are suited for including in solid MN composition [96,97]. A distinct microfabrication technique is employed to process a particular material.

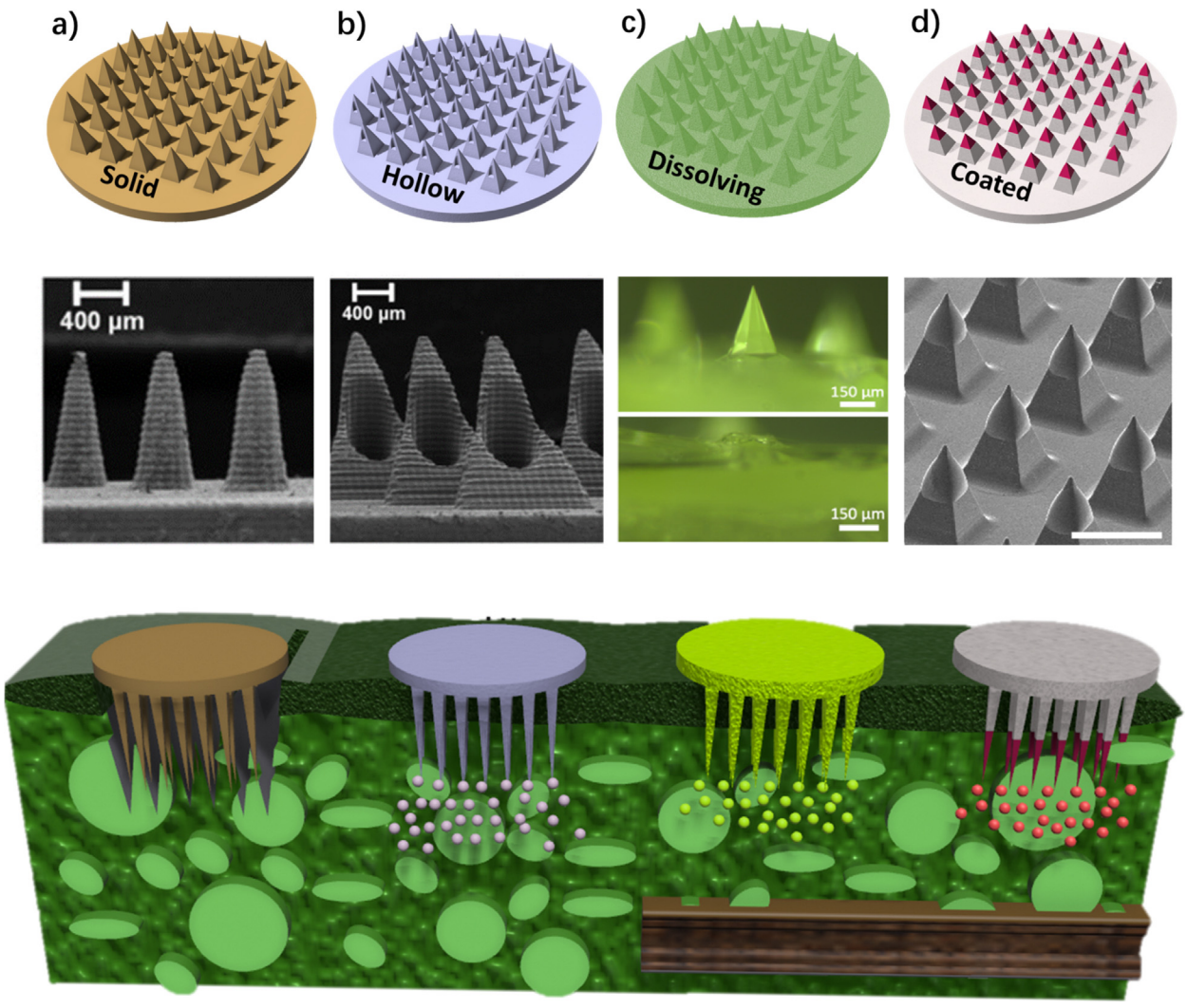

FIG. 3

Types of microneedles (MNs) with fabrication and sensing-treatment applications on plants were illustrated. (a,b) SEM images of solid MNs and hollow MNs were were exhibited. Reprinted with permission [149]. Copyright 2011, Wiley. (c) Optical images of dissolving MNs were displayed. Reprinted with permission [213]. Copyright 2022, Elsevier. (d) Images of coated MNs were captured using SEM, fluorescence and optical methods. Reprinted with permission [214]. Copyright 2022, Scientific Reports.

Microelectromechanical systems (MEMS) technology is promising for manufacturing solid MNs with optimal design parameters for agricultural applications [26]. However, the process is complex and requires cleanroom procedures involving photolithography, thin film deposition, and etching [98]. Although the outcome is highly precise, MN manufacturing can be laborious, time-consuming, and costly. Hence, cleanroom-free fabrication approaches such as CO_2 laser cutter [84], microinjection molding technique [99], hot embossing [100], electroplating [101], drawing lithography [102], a combination of micromilling and spray deposition [103], two-photon polymerization [104], and 3D printing techniques [16] have been exploited (Fig. 4**a**-**h**).

Solid MNs in agriculture face limitations due to the need for repeated and multiple applications, which is laborious in the field. One solution is to increase the density of MN arrays on a single patch, allowing for the delivery of a higher amount of agrochemicals [105]. Li et al., for instance, have investigated the impact of different polylactic acid (PLA) solid MNs with varying densities on drug release rates [106]. The amount of the delivered drug using MNs with the density of 100, 144, 196, and 256 MNs/cm^2 were 152, 210, 284, and 418 ng/cm^2, respectively. Another setback in using solid MNs is that the pierced pores can quickly heal, limiting the sufficient delivery of agrochemicals. Moreover, owing to the risk of infections in the pierced area [107], solid MNs have not been usually preferred MN types for agricultural applications. From this direction, the demands for new varieties of MNs have grown. Regardless of the aforementioned limitations, the design of solid MNs is particularly vital since they are used as a template for further manufacturing of coated and dissolving MNs.

Hollow microneedles

With the improvement in microfabrication techniques, manufacturing MNs with hollow constructions has recently become far more prevalent [108]. These MNs are similar to the conventional hypodermic needles, with size decreased to micron scale. The hollow MNs, reliant on the "poke-and-flow" mechanism, operate with pressure-driven flow for the transportation of the

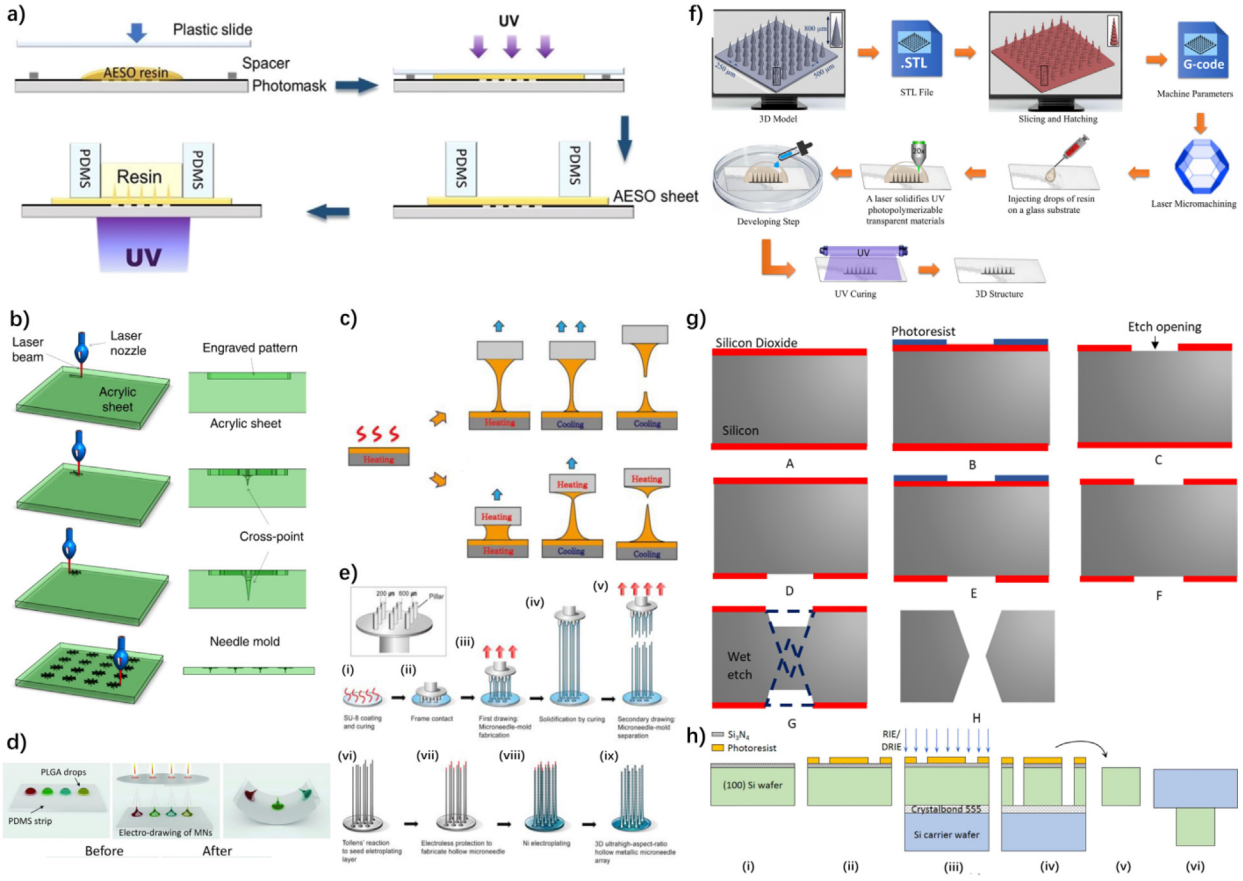

FIG. 4

Different microneedle (MN) fabrication methods were demonstrated. (a) Fabrication of MN arrays via inverted light UV lithography was illustrated. Reprinted with permission [215]. Copyright 2021, American Chemical Society. (b) CO_2 laser cutter was utilized to fabricate MN acrylic mold using the proposed cross-over lines (COL) technique. Reprinted with permission [84]. Copyright 2018, Springer Nature. (c) Conventional thermal drawing and spatially discrete thermal drawing were employed to fabricate MN. Reprinted with permission [216]. Copyright 2013, Elsevier. (d) Electron-drawing method was applied to obtain MN. Reprinted with permission [217]. Copyright 2014, Wiley. (e) MN arrays were designed and fabricated using lithography. Reprinted with permission [102]. Copyright 2010, Wiley. (f) MN were produced using 3D printing and laser solidification, respectively. Reprinted with permission [218]. Copyright 2022, Elsevier. (g) In-plane silicon MN fabrication method with cross-section of process steps was demonstrated. Silicon wafers, silicon dioxide, and the photoresist were represented in grey, red, and blue, respectively. Reprinted with permission [219]. Copyright 2022, Elsevier. (h) Deep reactive ion etching (DRIE) and photolithography were used for MN production. Reprinted with permission [220]. Copyright 2022, Elsevier.

drug/sample through the reservoir at a steady rate [109]. Hollow MNs can be employed in drug release and detection studies by either administering or collecting the required drug/samples (Fig. 3**b**) [110]. Silicon [111], metal [112], polymeric [113], and glass materials [114] are extensively used in fabricating hollow MNs [115]. MEMS technique followed by deep reactive ion etching (DRIE) is conventionally used for MN fabrication in large quantities. 3D laser lithography [116], micro-stereolithography [117], CNC machining [118], and UV lithographic processes [119] have been also employed in design and fabrication of hollow MNs. Similar to dissolving MNs, hollow MNs are unsuitable for treatment and prevention purposes in agriculture. The use of hollow MNs in agricultural products is highly limited. Such MN systems have been previously applied on surfaces of leaves, stems, and petals to electrochemically detect *p*-cresol, a phenolic substrate that is essential to evaluate the biofuel potential in plants [120]. Although their application in agriculture is not common, they can be potentially integrated into agricultural products as a detection tool. As an advantage over coated MNs, which are widely used in agriculture, hollow MNs can extract a volume of sample that is orders of magnitude higher than other types of MNs, which can drastically improve the limit of detection and accuracy of the analysis. Hollow MNs can be used for a range of applications beyond just detection, particularly for drug delivery, benefiting to precision agriculture.

Dissolving microneedles

Due to their superior properties, including high drug loading capacity, simple manufacturing, and facile usage, the dissolving MNs have garnered notable attention in recent years [14,121]. Such MNs complement the "poke-and-release" strategy and are generally used in drug delivery rather than biosensing applications [122]. In brief, drugs are loaded into MNs, which are then dissolved upon penetration into target tissues and released in a controlled manner (Fig. 3**c**) [123]. Their fabrication usually involves a two-step process [124]. A solid MN is first manufactured using aforementioned technique in section 3.1.1. and used as a male template. Then, a polymer, typically polydimethyl-

TABLE 1

Microneedles in Detection Applications.

Agricultural Product	Part of the Plant	Targetted Molecule/Process	Purpose of Process	Microneedle Type	MN Properties	Fabrication Method	Detection Limits and time	Analyzing Tool	Highlights	Ref
Tomato	Leaf	*Phytophthora infestans*	Late Blight Disease	Polyvinyl alcohol (PVA) solid MN	Height of 800 μm, base diameter of 300 μm, and a tip diameter of 10 μm.	PDMS master mold fabricated using laser ablation and used as a template.	~60 min detection time	qPCR	Reducing chemical usage and time consumption and more DNA extraction in comparison to CTAB.	[24]
Tomato	Leaf	*Phytophthora infestans* and tomato spotted wilt virus (TSWV)	Late Blight Disease and bronzing in leaves	Polyvinyl alcohol (PVA) solid MN	Height of 800 μm, base diameter of 300 μm, and tip diameter of 10 μm.	PDMS master mold fabricated using laser ablation and used as a template.	~30 min detection time and 1 pg DNA detection limit	LAMP and monitoring system with smartphone integration	Real-time monitoring. DNA storage capability on MN surface for up to 3 days. Low detection limits.	[156]
Citrus macrophylla	Leaf	Green fluorescent protein (GFP)	Understanding plant mechanisms under stress	Titanium (Ti) solid MNs (Dermaroll)	Height of 250 μm.	N/A	N/A	Western Blot Analysis and Confocal Microscopy	Enhancing agrobacterium infiltration efficiency.	[188]
Orange and Kiwi	Fruits	Gallic acid (GA) and chlorogenic acid (CA) - Polyphenols	Measurement of the amount of antioxidants and understanding of plant physiology	CNT-CNC-GOPS coated MN	Height of 700 and base diameter of 40 μm	CNT-CNC coated (silylated) MNs are coated with GOPS using the LBL technique.	0.29 ± 0.2 μg/mL for GA and 0.34 ± 0.2 μg/mL	Cyclic Voltammetry (CV) method	Different CV values at different depth points demonstrate varying antioxidant levels and contents.	[25]
Arabidopsis, grapes, and radishes	Vegetables, fruits and their squeezed juice samples	Abscisic acid (ABA) hormone	Understanding of abiotic stress, defense mechanism against pathogens, and regulating developmental processes	Au@SnO2-vertical graphene coated MN	Height of 600–620 μm	SnO_2 sputtered tantalum (Ta) wires coated with graphene and gold nanoparticles, respectively.	0.012-495.2 μM concentration and 4–7 pH range	Amperometric response	High pH and concentration detection range, minimal invasiveness, and ongoing-plug in method for the ABA detection.	[27]
Tomato	Stem and xylem sap	Water transportation	Monitoring the physiological condition of a hydroponic plant	Ti-Au coated MN	Height of 300 μm and width of 500 μm	Silicon substrate coated with Ti and Au layers, and the MN structures were formed via deep reactive ion etching.	N/A	Printed circuit board (PCB) for fixing the MN and a connector for electrical conductivity.	Revealing of important association between solar radiation and sunlight, humidity, and soil water.	[26]

(continued on next page)

TABLE 1 (*CONTINUED*)

Agricultural Product	Part of the Plant	Targetted Molecule/Process	Purpose of Process	Microneedle Type	MN Properties	Fabrication Method	Detection Limits and time	Analyzing Tool	Highlights	Ref
Tomato	Stem	Ions and nutrients	Electrical conductivity quantification for ion balance in a plant	Silicon MN sensor	Height of 200 μm	Silicon MN was fabricated using the MEMS fabrication process.	2–100 kHz frequency range of AD5933 chip	Printed circuit board (PCB) for fixing the MEMS chip and AD5933 for impedance converter	Water and nutrient supplies affected the electrical conductivity and plants' reaction to the environmental conditions was demonstrated.	[29]
Arabidopsis thaliana	Leaf	Light exposure	Understanding, regulating, and controlling photosynthetic processes	Ti-Au Coated MN	Height of 400 μm and base diameter of 70 μm. 20 times reusable.	Silicon master was fabricated using two-photon polymerization (TPP) and coated with Parylene C. Cured PDMS mold was coated with titanium and gold.	N/A	Electrical impedance spectroscopy (EIS) for evaluation of structural alterations and physiological conditions of a plant	12-day light exposure results facilitated the understanding of photosynthetic processes and assessment of the water content of plants.	[143]
Tomato	Leaf	pH measurement with quinone groups	Analysis of physiological condition and defense mechanisms of a plant using a reaction between quinone groups and carbon nanoparticles	Carbon-loaded polystyrene MN	Height of 700 μm and a base diameter of 200 μm.	Carbon nanoparticles and polystyrene powder were mixed and cured on the silicon MN master mold.	N/A	Cyclic Voltammograms (CV) for pH measurement	Carbon fiber stub for enhancing the electrical connection. Quinone groups and carbon NPs caused pH changes. Continuous pH monitoring	[164]
Arabidopsis thaliana	Leaf	Physical damage	Understanding the pathogenic defense mechanism with stimulating actin cytoskeleton by utilizing physical damage	Tungsten MN	1–5 μm tip diameter and 1000 μm base diameter.	N/A	500–1000 nm penetration depth range	Confocal microscope to visualize the penetration level of MN and the expression of GFP	Force of 4 N have exposed for 22 s and the average reaction time was obtained as 48 s.	[167]

TABLE 1 (*CONTINUED*)

Agricultural Product	Part of the Plant	Targetted Molecule/Process	Purpose of Process	Microneedle Type	MN Properties	Fabrication Method	Detection Limits and time	Analyzing Tool	Highlights	Ref
Barley	Leaf	Bioimpedance measurement	Bioimpedance analysis for monitoring the photosynthetic process and the water necessity under 12 h of light and 12 h of darkness	Ti-Au coated MN	Flexible MN sensors with 500 μm and 230 μm lengths and 240 μm base diameter	Silicon master mold fabricated using TPP and coated with Parylene C. Cured PDMS coated with Ti, nickel (Ni), and Au after applying O_2 plasma.	N/A	A potentiostat is attached to record bioimpedance analysis	Higher bioimpedance values during the light because of the increase in photosynthetic activity and diffusion of water to the phloem.	[168]
Soil	Soil	Nitrate concentration	Quantification of Nitrate concentration to observe the soil richness	Au-Copper (Cu) coated MN	Electrochemical sensor-based MN with wireless communication integration	N/A	Limited to a minimum 100 nM nitrate solution	A counter electrode (CE), working electrode (WE), and reference electrode (RE) was utilized for the detection and measurement of electrical properties.	The ion level and soil richness can be detected. Nitrate concentration was measured between 15 and 80 μM.	[144]
Catharanthus roseus	Leaf, Stem, and Root	Catharanthine and vindoline - anhydrovinblastine	Determination of anhydrovinblastine content that is used for cancer therapeutics	Commercial product Stainless steel MN	Diameter size of 100 μm and length of 1000 μm MN	Purchased MN was heated at 1000 °C to obtain surface oxidation. Signal intensity was enhanced using strong-acid treatment (SAT).	N/A	Mass spectroscopy (MS) for chemical analysis of catharanthine and vindoline	Catharanthine and vindoline which form anhydrovinblastine obtained in stem and leaf. In the roots, the vindoline molecule was not detected, while catharanthine was measured.	[170]

TABLE 2

Microneedles in Delivery Applications.

Agricultural Product	Part of the plant	Targetted Molecule/process	Purpose of process	Microneedle Type	MN Properties	Fabrication Method	Detection Limits and time	Analyzing Tool	Highlights	Ref
Young Valencia orange saplings	Stem – phloem tissue	*Candidatus Liberibacter* asiaticus (CLas)	Transportation of novel therapeutics for Huanglongbing (HLB) disease	Cu NPs coated MN	Height and base radius of 2000 and 500 μm	Digital light processing (DLP) 3D printed resin-based MN was coated with Cu NPs using sodium oleate	N/A	Energy dispersive spectroscopy (EDS) and SEM were employed for characterization of released Cu NPs	Phytotoxicity-free Cu NPs as a model were transported to phloem tissue to inhibit the targeted pathogens	[22]
Citrus saplings	Stem	Agrochemical transportation	Zinkicide delivery for assessment of penetration of MN and delivery of agrochemical	Solid stainless steel micro-milled MNs (μMMNs)	Base width and height of 500 μm	The fabricated planar MN arrays were turned into 3D structures using Hypo-Rid	N/A	Atomic absorption spectroscopy (AAS) for the measurement of the amount of zinc in the stem	The amount of zinc was measured to evaluate the delivery of Zinkicide. Zinc molecules have been obtained in the close regions to the phloem	[18]
Arabidopsis thaliana and soybean	Leaf and shoot apical meristem (SAM)	Delivery of Cre recombinase and Cas9 ribonucleoprotein (RNP)	Delivery of genome-editing proteins without undesirable genetic changes to enhance the functional quality of plants	Silicon-based solid MN	MN arrays (MNAs) with 40 μm, 60 μm, and 100 μm height	Patterns were obtained on the silicon-on-insulator (SOI) wafers using photolithography. Using a photomask, the size properties of MN arrays were altered.	N/A	Fluorescence microscopy for imaging the expression and Next-generation sequencing analysis for assessment of PDS11/18 through the delivery of Cas9 RNP	Delivery of these genome-editing proteins was accomplished in leaf parts of different plants.	[182]
Tobacco and tomato	Leaf and shoot apical meristem (SAM)	Delivery of agrobacterium-mediated genes	Delivery of payloads to enhance the resistance of plants to biotic and abiotic stress	Rhodamine 6 g and azoalbumin loaded Silk Fibroin (SF) - α-chymotrypsin (Cs) MN	20:80 Cs-SF MN with a height between 100 and 200 μm	PDMS mold was poured and cured using Al master. Cs-SF solution was mixed with payloads and cured.	The limit ratio for Cs was determined 20% to obtain optimum solubility	Fluorescence microscopy for imaging the green fluorescence protein (GFP) expression	Delivery of agrobacterium genes into SAM and leaves demonstrated the penetration capability of MN with controlled dissolving.	[184]

siloxane (PDMS), is poured on the male template to form female PDMS molds, which then left on a hot plate at a temperature of around 80 °C for approximately 2 h to cure. Finally, a polymer solution is poured over the cured female PDMS mold and polymerized at certain conditions. These conditions usually include monomer concentration, cross-linking agents, temperature, solvent, and polymerization time. For example, monomer concentration affects the degree of polymerization. Cross-linking agents can be included to enhance the mechanical properties and stability of the polymer. The temperature factor has direct impact on polymerization rate. Lower temperature values usually result in slower polymerization rate, and this eventually lead to incomplete polymerization. Although the polymerization occurs more quickly at higher temperatures, it may lead to the formation of unwanted side products. The solvent selection impacts the solubility of monomer and the polymer mixture, altering morphology and mechanical feature of the resulting polymer. The total length of time allowed for polymerization reaction drastically change the molecular weight distribution and the degree of polymerization. Longer polymerization time can cause certain degradation in polymer. Hence, these conditions should be selected carefully depending on the nature of the polymer. After the desired polymerization occurs, the dissolving MNs are then formed by peeling off the cured polymer from the PDMS surface. During the curing process, photopolymerization can be employed to speed up the process [125]. Other techniques such as micro molding [126] and drawing lithography [127] have also been conducted for such synthesis. They are also considered polymeric MNs; hence, they have drawn attention to polymer-related research [128]. Water-soluble, smart materials and biodegradable polymers (e.g., gelatin and polyvinyl alcohol (PVA)) are the most frequently used materials [129]. Hollow MNs are biocompatible, dissolve without leaving harmful materials, and can achieve zero-order drug release [130]. However, their use in agriculture is limited due to the difficult synthesis and high cost of polymers, making reusability infeasible.

Coated microneedles

Coated MNs operate based on the "coat-and-poke" mechanism and can be employed both as delivery and biosensing tools. They are manufactured by immobilizing coating agents on MN tips [131]. Compared to the poke-and-patch approach (solid MNs), delivery or detection processes can be accomplished in a single step (Fig. 3**d**) [123]. The geometry and size of the MN arrays are fundamental as they affect the amount of coating agents to be immobilized on the surface [132]. Once they interact with the interstitial fluid of a plant, the coating agent is either released from the MN tips to treat a disease or capture a signal (i.e., chemical and electrochemical) to detect infections or toxin levels [133]. The fabrication methods in their designs are similar to the ones used in solid MNs. Different from solid MN, their fabrication involves a second immobilization step. Numerous coating processes have been reported in the literature [134–136]. The most common coating methods are dip-coating [137], inkjet coating [138], immersion coating [139], drop coating [140], and spray coating [141]. That being the case, materials need to be carefully chosen as the interactions between MN material and coating agent determine drug loading capacity or biosensing

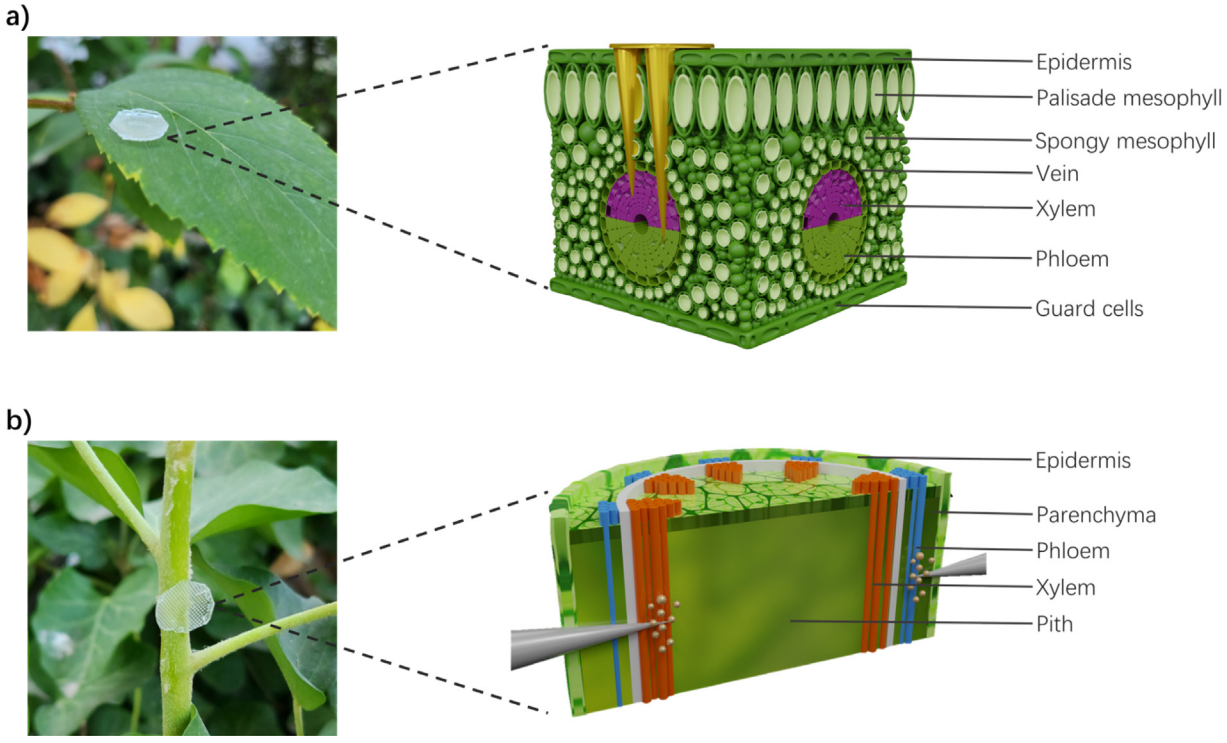

FIG. 5

Microneedle (MN) insertion into the plant leaf and stem was demonstrated. (a) Polyvinyl alcohol-based MN patch was inserted into the leaf of *Deutzia scabra* (left) and the illustration of MN penetration into the plant leaf (right). (b) MN patch was inserted into the stem of *Hedera colchica* (left) and the illustration of MN insertion into the plant stem (right).

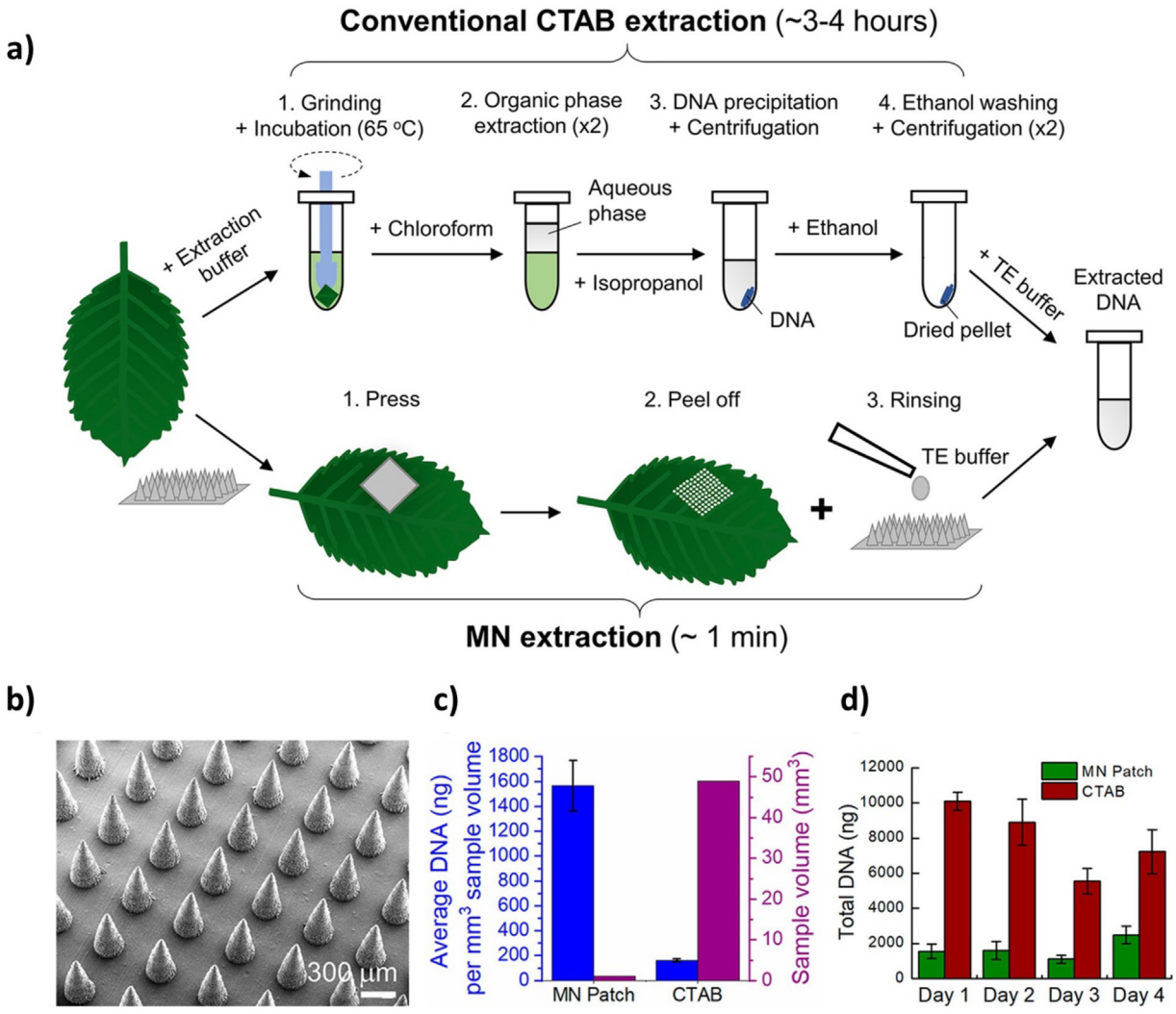

FIG. 6

A DNA extraction method through microneedles (MNs) was demonstrated. (a) Comparison of the duration of extraction and chemical consumption between conventional CTAB extraction and MN extraction were illustrated. (b) SEM image and optical image of the MN patch were exhibited. Scale bar: 300 μm. (c) The amounts of total DNA extracted by two extraction methods (blue bars) were measured, revealing 8 times higher extraction efficiency of the MN method. The difference in sampling volumes of the methods were represented with purple bars. (d) Average amount of total DNA was calculated using MN patch and CTAB methods for different inoculation days. While the total amount of DNA decreased day-by-day in the CTAB method, this rate was maintained in the MN method. Reprinted with permission [24]. Copyright 2019, American Chemical Society.

precision. Up to date, materials such as *Francisella novicida* bacterium [142], nanocomposite of carbon nanotubes and cellulose nanocrystals [25], titanium/gold [143], Au@SnO_2-vertical graphene [27], and gold/copper [144] have been utilized as coating agents for detection purposes in plants. Using the coated MNs, a wide range of conditions including polyphenol levels, water transportation efficiency, light exposure, bioimpedance, nitrate concentration, and hormone levels have been measured and monitored in plants (see Tables 1 and 2).

Overall, MN technology is a promising tool to hurdle the limitations encountered in conventional techniques and their implementation in agriculture. Prompt, precise, and more environmentally-friendly technologies are indispensable for a more feasible vision for the future of agriculture. The MN technology keeps growing with increasing number of studies in detection and therapeutic investigations. The application of MNs in animals as a delivery and detection tool is widely explored, and several reviews have discussed the use MNs in such events [145–150]. Herein, we will present the application in agricultural products.

Microneedles as a detection implement in agriculture

It is common to use MNs for determining disease-causing substances in agricultural products, screening of physiological conditions in plants, and other essential chemicals. MNs are either utilized directly as a biosensor or for on-site extraction of chemical elements that needs to be further characterized through downstream analyses. These platforms have been diversified depending on MN type, the properties of the plant site to which the MNs will be applied (i.e., hardness, thickness, fragility), and the properties of the substance to be detected (i.e., water solubility, hydrophobicity) (Fig. 5). In this section, the use of MN

technology as a detection platform will be introduced as shown in the timeline (Fig. 1).

Plant disease monitoring and pathogen detection

It is crucial to swiftly identify highly infectious pathogens [151–153] that can spread from host plant and contaminate healthy plants. This extensive infectiousness, similar to the current pandemics, might not only drastically lower agricultural productivity, but also be harmful to both human health and nature. With the use of MN technology, a rapid and direct analysis will be performed where the disease is present; hence preventive measures can be taken effectively and rapidly.

As an example, nucleic acids have been primary targets in determining several plant diseases and can be detected using MNs. In this regard, Paul et al. carried out the detection of pathogenic DNA from *Phytophthora infestans* in tomato leaves by using a MN system without cell fragmentation and purification process (Fig. 6**a**) [24]. Briefly, in this study, MNs were manufactured using polyvinyl alcohol (PVA). The template to manufacture polydimethylsiloxane (PDMS) mold, which was utilized for PVA MN production, was fabricated using laser ablation, and PVA MNs with a length of 800 μm, base diameter of 300 μm, and a tip diameter of 10 μm were obtained (Fig. 6**b**). Tomato leaves were then treated with MNs, and the MN surface was

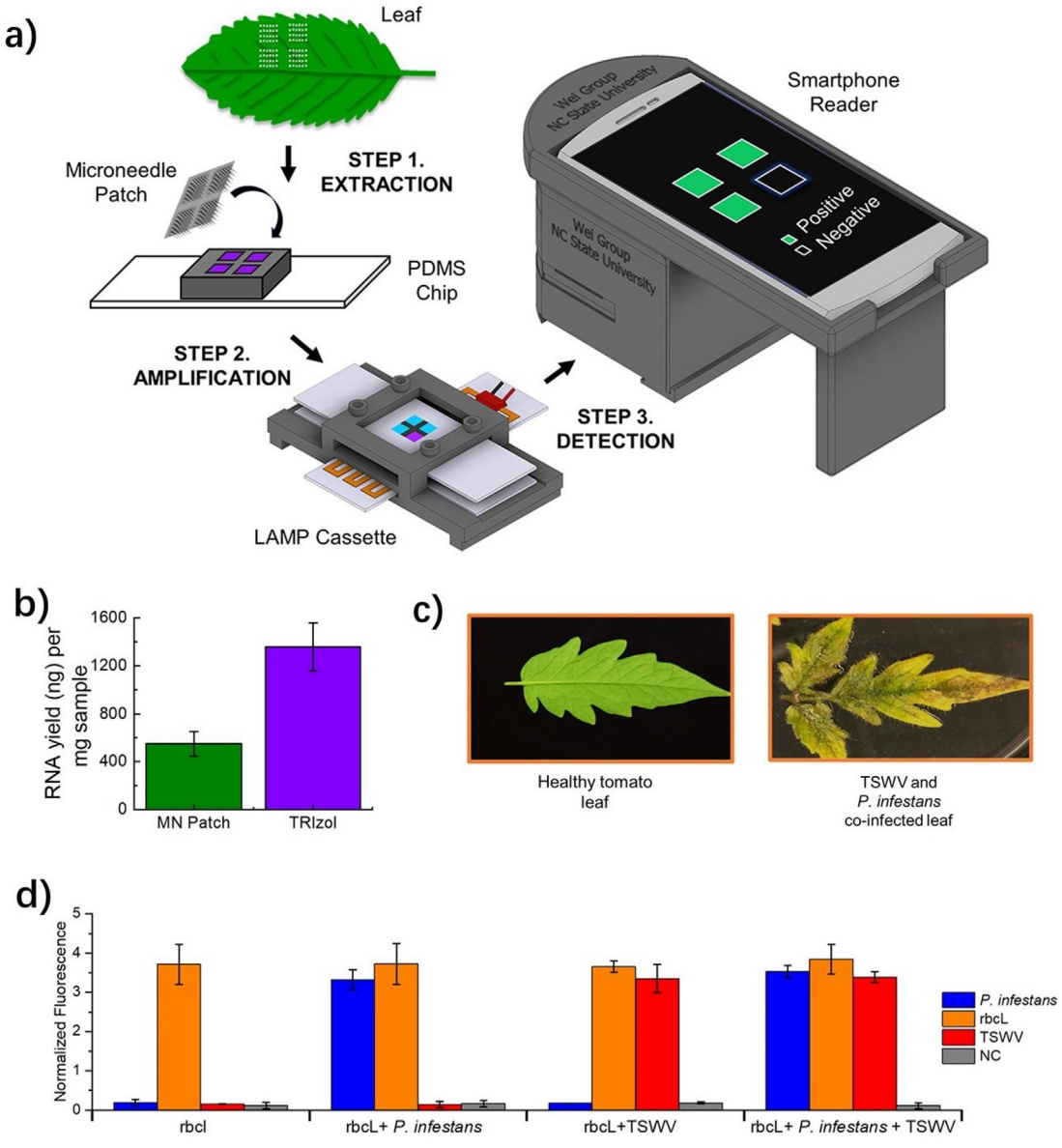

FIG. 7

Microneedle (MN) extraction and LAMP employment for pathogenic DNA detection were demonstrated. (a) DNA extraction process using MN patch and amplification-monitoring steps with LAMP integrated smartphone were shown. (b) Total extracted RNA yield was measured as 600 and 1400 ng/mg sample for MN patch and TRIzol method, respectively. (c) Leaves with healthy and co-infection (*Phytophthora infestans* and TSWV) were captured using smartphone. (d) Normalized fluorescence values of *Phytophthora infestans* and TSMV were measured. The fluorescence analysis was evaluated for each set of experimental condition. Reprinted with permission [156]. Copyright 2021, Elsevier.

washed with Tris-EDTA buffer upon the removal of MNs for separating pathogenic DNA adhered to the MN surface. Approximately 200 and 1600 ng/mm^3 of DNA per sample volume have been extracted using cetyltrimethylammonium bromide (CTAB) method and MN approach, respectively (Fig. 6**c**). On the other hand, total amount of extracted DNA was consistent with the MN implementation for 4 days, while the CTAB implementation demonstrated unstable DNA extraction within this period (Fig. 6**d**). The cycle threshold (Ct) value, which expresses the total number of cycles required to amplify the pathogen DNA [154], was calculated using quantitative polymerase chain reaction (qPCR), and the MN approach was only five cycles higher than the CTAB method. Replacing the CTAB method with the MN approach eliminated the use of organic solvents, bringing affordable and ecological advantages. The designed system provided the results in ca. 1 min while the CTAB method took 3–4 h. Such a reduction in the detection time of this pathogen that causes late blight disease is of great importance. Executing such pathogen detection studies more quickly is critical, especially for pathogens that rapidly infect other plants and organisms. In addition, with the integration of portable PCR devices recently performed by other researchers [155],portable systems can be obtained and used in-field.

On a parallel track, Paul et al. presented a MN technology, which was combined with the rapid and comprehensible features of smartphone technology to monitor fragile plant RNA, and DNA molecules were amplified using loop-mediated isothermal amplification (LAMP) (Fig. 7) [156]. Herein, conical PVA MNs were produced with a similar method exhibited in previous study [24]. Each patch had a total of 225 MN arrays with a height, tip, and base diameter of 800, 10, and 300 μm, respectively. Furthermore, DNA could be stored on MN surface for up to three days without degradation. Nucleic acids were extracted from tomato leaves in about a minute following the removal of MN patches. DNA and RNA samples were delivered to the assay cassette, which was used for the LAMP test, connected to a smartphone reader (Fig. 7**a**). The implementation of TRIzol, which is a conventional RNA extraction strategy, were conducted for the comparison with MN performance and demonstrated the higher amount of extracted RNA, while causing huge physical and chemical damage on the contaminated leaf samples. As a result, extracted RNA yields were measured as 600 ng/mg sample and 1400 ng/mg sample for MN patch and TRIzol, respectively (Fig. 7**b**). In-field study showed a reliable method for identifying *P. infestans* and tomato spotted wilt virus (TSWV) on tomato leaves with diagnosis time reduced to ~ 30 min (Fig. 7**d**). Moreover, this platform was able to detect DNA of TSWV and *Phytophthora infestans* from tomato leaves down to 1 pg/μL. These studies also showed the potential use of MNs in LAMP assays, as well as their integration with smartphones to adapt the technology to be applied at point-of-need. In addition, studies focusing on machine learning can be included to improve the detection

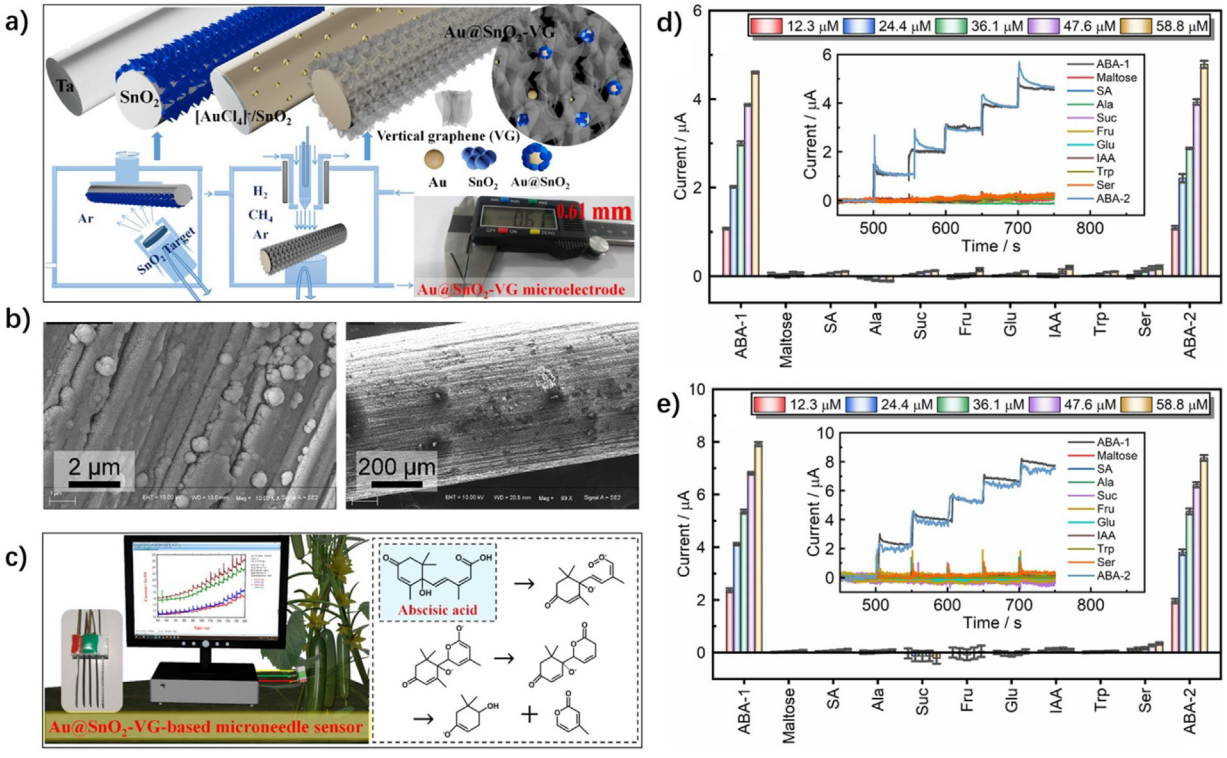

FIG. 8

Au@SnO2-vertical graphene-coated microneedles (MNs) were fabricated for the detection and measurement of abscisic acid (ABA). (a,b) Illustration of MN production process and its application for the detection of abscisic acid (ABA) were demonstrated. (c) The integration of MN platform with a computer for ABA analysis were illustrated by indicating the molecular structure of ABA.(d) The results of the MN array sensor for ABA at pH 4.5 were plotted. These results indicated the selectivity of MN sensor for ABA analysis. (e) At pH 6.5, MN array provided a detection range within 12.35–58.8 μM concentration. The sensitivity of the MN sensor was demonstrated between specific concentration range and at different pH levels. Reprinted with permission [27]. Copyright 2021, Elsevier.

capabilities of such platforms and to obtain more precise and standardized results. In this way, the intensity of fluorescence can be analyzed instantly, and plant diseases that show different fluorescence characteristics at different stages can be predicted and chased more precisely [157]. On the other hand, as mentioned in the previous study, such a shortening of the time is of vital importance for the rapid detection of pathogens with the potential to spread.

Metabolite monitoring

Crucial components such as primary and secondary metabolites extracted from plants play key role in their defense mechanism. For instance, polyphenolic compounds take part in the defense mechanism against UV radiation and pathogens while organic acids determine the agri-food quality [158,159]. Dhanjai et al. have introduced stainless steel MN electrode (40 mm × 700 μm) to detect polyphenols, including gallic acid (GA) and chlorogenic acid (CA) using orange and kiwi samples [25]. MN was first modified with active hydroxyl moieties followed by silylation with 3-(trimethoxysilyl) propyl methacrylate (TPM)/water/Methanol solution to chemically bind organosilane to the MN surface as polymer anchoring moiety. Carbon nanotubes (CNT) and cellulose nanoparticles (CNC) were coated on modified MNs, respectively. Redox reaction-based analysis was executed with MN electrode upon insertion into orange and kiwi samples. Quantification of CA and GA antioxidants in orange and kiwi was performed using Cyclic Voltammetry (CV) method. The CV values in orange and kiwi were recorded differently at depth points varying between 25 and 33 mm and 7 and 26 mm, respectively. The LOD values for GA and CA were 0.29 ± 0.2 μg/mL and 0.34 ± 0.2 μg/mL, respectively. The fabricated MN electrodes exhibited prodigious reproducibility for 14.29 μg/mL CA and 14.51 μg/mL GA as 0.95% relative standard deviation (RSD) and 2.25% RSD, respectively. As a consequence, the GA and CA chemicals were detected as 57 ± 3 μg/mL and 48 ± 4 μg/mL from orange juice, respectively. The approximation of the results with standard solutions validated the reliability of this study and its potential for use in other fruits. Further studies such as monitoring these antioxidants instantly during the day and examining their changes depending on sunlight and humidity would be carried out. In addition, soil quality would be assessed at the same time by conducting the determination of chemicals from the soil. In addition, all these systems can be monitored remotely with wireless integration and the necessary systems (i.e., irrigation, drying, spraying) can be activated instantly [160].

The plant hormone abscisic acid (ABA) defends plants against various pathogens, responses to abiotic stress, and regulates developmental processes (i.e., stomatal closure and seed germination, and stopping plant growth) [27,161,162]. As an example, Wang et al. developed an MN sensor based on Au@SnO_2-vertical graphene for in situ detection of ABA content in cucumbers by direct electrocatalytic oxidation (Fig. 8) [27]. For MN fabrication, SnO_2 was first sputtered on tantalum wires (0.6 mm × 7 mm) using magnetron sputtering system, which was followed by embedding vertical graphene nanolayers with $HAuCl_4$ solution to obtain gold nanoparticles on the surface (Fig. 8**a,b**). MN array sensor efficiently responded to ABA concentrations (0.012-495.2 μM) within a range of pH 4 – pH 7 by using an effective electroactive surface area spanning from 0.13 cm^2 to 0.53 cm^2. The LOD value for ABA detection was between 0.002 μM and 0.005 μM. The MN sensor presented good stability during five-month storage at room temperature. The RSD value, which determines the sensitivity of the MN array sensor, was measured as 3.65%, and the ABA concentration range was quantified between 24.6 and 117.6 μM. The selectivity test of the produced platform was measured by the addition of biomolecules to the medium during measurement, and negligible changes of 0.6% and 1.7% were observed at pH 4.5 and pH 6.5, respectively. This technique would be extended to deeper tissues by varying the lengths of MN tips and would be easily implemented into an online monitoring system. That online monitoring system also can be integrated with wireless technology for conducting and analyzing measurements remotely [163].

Monitoring physiological condition

In agriculture industry, understanding of physiological conditions of plants is pivotal to improve the sustainability of harvesting practices and increase the crop yield. The monitoring of water transportation in xylem sap flow provides information regarding the current physiological condition of the plant. This process is carried out in plant stem to control the responses of plants against altered environmental conditions (i.e., sunlight, humidity, soil water). For instance, Baek et al. have developed a MN thermal probe to measure water transportation in tomatoes grown in hydroponics [26]. The MN sap flow sensor was manufactured using MEMS fabrication technique. Silicon MN arrays with a 500 μm width and 300 μm thickness were formed using deep reactive ion etching. In the final step, silicon MNs were combined with a printed circuit board (PCB) and the connector. MN sensor was applied for 36 days to continuously measure in vivo signal acquired from tomatoes. The results of every MN were compared and the margin of error was calculated as 10%. The findings revealed a significant association between the diurnal cycle of the plant (circadian clock) and solar radiation and air temperature. MN probe presented less error range than other thermometric measurement of sap flow. However, at the end of 36 days, 20% of sensors failed due to mechanical breakage. With this study, a crucial step has been taken in in-field measurements. Increasing the mechanical strength, on the other hand, can provide more accurate results by implementing more MN. Turning this study into a chip-based system and tracking it simultaneously for long periods in many regions of the world would be a mainstay forward in examining the causes of climate change, in addition to monitoring the health status of plants. In this way, wider measures can be taken for the coming years for a greener earth.

Nutrients, which are crucial for crop growth, have a considerable impact on the ion balance in plants. The impedance measurement is widely utilized to determine ion balance by monitoring electrical conductivity (EC). The control of salinity of these nutrients is crucial to maintain healthy horticultural crops such as tomatoes. However, any damages on crops are inevitable during such analyses, and more precise results would be obtained once agri-food has reached certain maturity. To overcome these drawbacks, a MN sensor has been developed by Jeon

et al. for real-time measuring the EC with minimal invasiveness [29]. The EC inside tomato stem was measured using an impedance measurement system. MN-based sensor system was constructed using similar method as previously described [26]. It has been observed that MNs shorter than 200 μm during application need a support during penetration. For MNs of 200 μm and longer, penetration was successfully accomplished without support. MN sensor was inserted into the tomato stem and the temperature changing and EC results were monitored in real-time for 45 h and 24 h, respectively. The MN-based device successfully measured EC due to the alteration in ion balance upon water and nutrient flow. The minimum EC value was measured as 1000 kΩ at 10.00 am. In addition to the change created by the plant's passive and active transport routes and liquid intakes in this value, it should be taken into account that the change in the air can affect this process as well as the sensor. With this study, taking measurements instantly has taken an important step in observing both plant health and soil quality. In another study, a MN-based sensor was fabricated by Bukhamsin et al. for long-term and reliable impedance measurement in *Arabidopsis thaliana* exposed to lighting and hydration [143]. The master mold was fabricated using two photon polymerization (TPP) laser lithography. Polyimide MNs with a height of 350 μm and a width of 70 μm, which were produced with this master mold, coated with 10 nm titanium and 150 nm gold after coating with SU-8/polyimide varnish *Phytophthora infestans*. Measurements resulting from changes in light and moisture were acquired after polyimide MN was inserted. It has been discovered that this MN product retained its conical shape after 20 uses. The analyses of the 12-day light exposure facilitated the understanding, regulating, and controlling of photosynthetic processes. That makes it essential to promptly and precisely assess the water content of plants to ensure their continued survival.

pH is another parameter influencing the quality of agricultural products and can be measured using MNs. Using carbon-embedded polystyrene MNs, Hegarty et al. have fabricated carbon-embedded polystyrene MNs to monitor pH in tomato flesh [164]. Carbon nanoparticles were loaded into the polystyrene MNs to provide conductivity between MN tip and base plate. MNs (700 μm × 200 μm), were coated with Enamel to be served as a dielectric. After measuring pH through cyclic voltammograms (CV) in tomato leaves, standard measurements using the Ag/AgCl traditional method were taken to compare MN performance. The presence of quinone groups at the interface of the embedded carbon nanoparticles could react to pH variations through redox transitions, functioning as a reagent-free pH sensor. pH values of 4.48 and 4.77 were measured for single MN (3 electrode) and dual MN (2 electrode) on a tomato skin, respectively. With standard measurement methods, these pH values were calculated as 4.43 and 4.52, respectively, and the fact that the difference was so low increased the reliability in the developed platform. This study could be used instantaneously in a wide range of fruit and vegetable products, and pH levels between pH 3.13 and pH 7.22 could be monitored continuously. This pH monitoring is especially critical for fruits and vegetables, which make a huge economic contribution worldwide. These pH levels need to be followed instantly and it need to be brought back to optimum levels in case of any change. In addition to these platforms where the pH level can be monitored, wireless can be integrated [165], and remote control can be provided by integrating platforms that can automatically adjust the pH level [166].

Plants can react to pathogens with physical responses, potentially manifesting the signaling pathways to induce plant immune system, which, in consequence, increase resistance against these pathogens. Branco et al. have developed a method to observe actin cytoskeleton response of *Arabidopsis thaliana* seedlings triggered by MN insertion that mimics attack of fungal or oomycete hyphae [167]. A glass or tungsten pyramid MN with a diameter of 0.25 μm was inserted with varying penetration depth (500 nm, 750 nm, and 1000 nm), hold time (0.5–4 min), and unload time (1–90 s). The response acquired from the plant cell wall varied depending on the aforementioned parameters. Green fluorescent protein (GFP) was utilized to define the structure of actin cytoskeleton in epidermal cells of hypocotyls. According to the results obtained with single-cell mass analysis, The actin microfilaments rearranged after being exposed to a force of 4 N for 22 s, and the average reaction time was 48 s. With the use of physical damage analysis, the findings of this study have improved our comprehension of how plants react to disease-causing agents.

Critical features in this concept such as small volume sampling, reliability, high accuracy, and reusability have made the use of impedimetric biosensors widespread. MNs can be integrated to these biosensors to confer flexibility and minimal invasiveness to the detection tool used to monitor crops. As an example, Bukhamsin et al. developed a flexible MN electrode system to measure bioimpedance in barley leaves under a controlled temperature and day/night cycle [168]. The master mold was fabricated using two-photon polymerization, and PDMS-based MN was produced using this master mold. PDMS MNs were coated with 40 nm of Ti, 5 μm of Ni, and 150 nm of gold, respectively. Two different flexible and light MN sensors were produced with lengths of 500 μm and 230 μm, each with a base diameter of 240 μm. Bio-impedance measurements, which were evaluated between 1 Hz and 100 kHz frequencies, were completed during 12 h of continuous illumination and 12 h of total darkness. When the light was turned on, the bio-impedance value increased dramatically. As a result of these analyzes that continued for 6 days, the impedance value increased from approximately 2.7×10^7 ohms to 4.3×10^7 ohms after the 3rd day. This may be due to the resealing process performed by the leaf on the MN. In general, the increase in impedance value between dark and light might due to strong photosynthetic activity in plants under light and the consequent diffusion of water molecules to the phloem. The fabricated MN-based electrodes were effective as an intelligent irrigation system in monitoring water requirement of barley crops. Determining the amount of water needed and giving it to the plants by remote control can not only protect the health of the plants, but also prevent unnecessary water consumption and protect the water [169].

Most plants contain bioactive compounds, which are employed in drug development. One of these substances is anhydrovinblastine—a single-cell metabolite and a key component of medications used to treat a variety of cancers. Cai et al., for instance, have utilized a stainless steel MN coupled to mass spectroscopy (MS) for extraction of anhydrovinblastine from *Catha-*

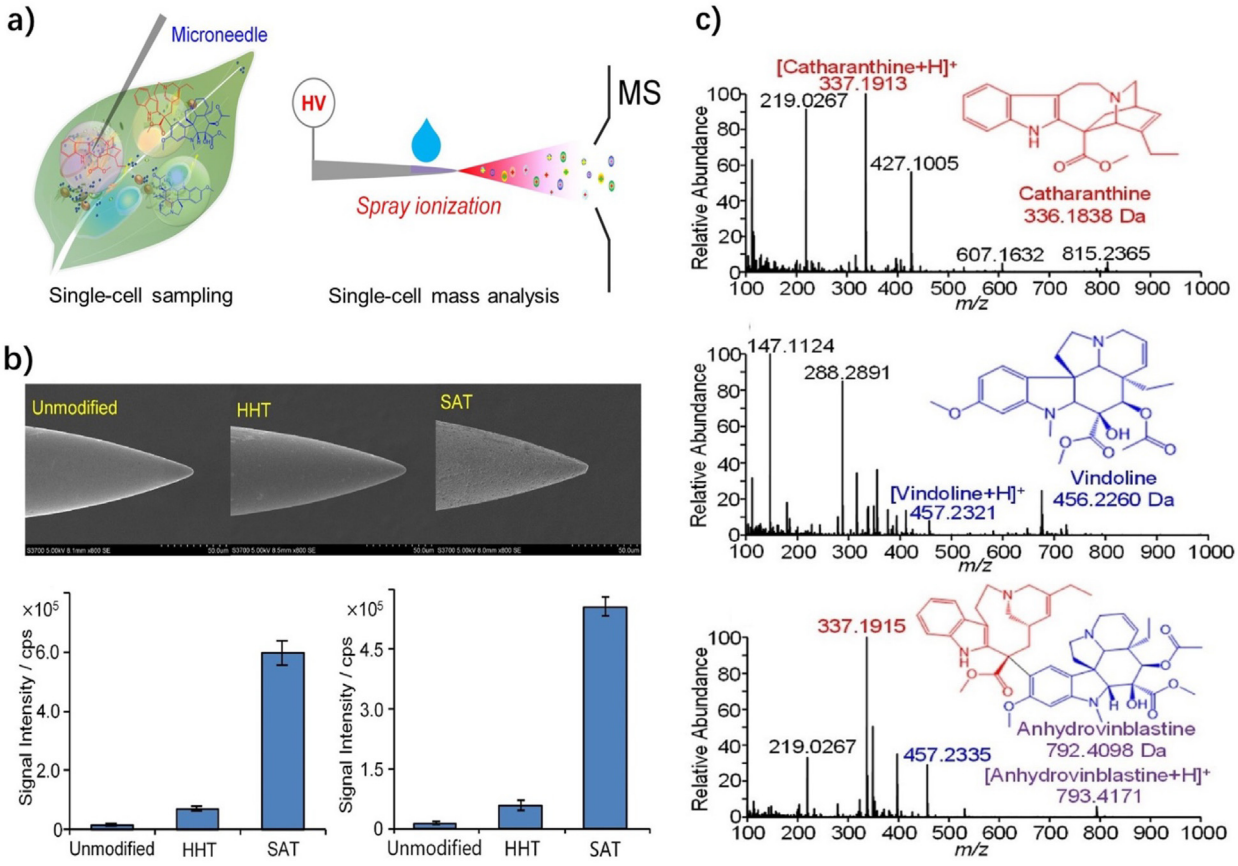

FIG. 9

Microneedle (MN) array with a strong acid treatment was fabricated for the detection and analysis of anhydrovinblastine. (a) MN sampling and direct analysis of single-cell metabolites using mass spectrometry (MS) were illustrated. (b) Metal MNs were imaged using SEM and compared with enhancing signal intensities. (HHT: high-temperature treatment; SAT: strong acid treatment) (c) Mass spectra result of single-cell metabolites: MS/MS spectrum of catharanthine (top) (337.1913 *m/z*), vindoline (middle) (457.2321 *m/z*), and anhydrovinblastine (down) (793.4171). With mass spectrometry analysis, three crucial components were detected and analysed by observing their relative abundance. Reprinted with permission [170]. Copyright 2022, Elsevier.

ranthus roseus (Fig. 9**a**) [170]. A commercially available metal MN (J15, Shizuoka, Japan) with an outer diameter of 100 μm and tip diameter of 1 μm was used to apply on plant. The MN was first heated to a temperature of more than 1000 °C to induce surface oxidation. The signal intensity of MN was then enhanced 42 times in comparison to the unmodified probe using strong-acid treatment (SAT) (Fig. 9**b**). Moreover, the limit of detection (LOD) value for catharanthine and vindoline was calculated as 1 ng/mL after treating the MNs with SAT. Additionally, SAT modified MNs demonstrated prodigious reproductivity as RSD < 10% of three repeating experiments. Vindoline and catharanthine compounds, which form anhydrovinblastine molecules as a result of their mixture, were detected from different cells. The protonated catharanthine peak at *m/z* 337.1914 and the protonated vindoline peak at *m/z* 456.2337 obtained upon insertion of MN into the stem have demonstrated that both compounds were present in the stem of *Catharanthus roseus* (Fig. 9**c**). MN applications in plant root did not sense any vindoline molecules, while the protonated catharanthine peak was observable. Both compounds as well as anhydrovinblastine were determined in the leaves. Moreover, upper part of the leaves was richer in catharanthine contents, while the lower part had higher amount of vindoline compound. Owing to this study, the determination of important molecules that will be used in the pharmaceutical industry was carried out with high accuracy. A machine learning method can be integrated to make the general analysis of the peaks taken from different regions of the plants faster and to make a general prediction by making a connection between the peaks [171]. Additionally, hollow MNs can be used to further extract the plant fluid containing these chemicals.

Soil composition such as mineral, water, and O_2 content greatly influences plant health and the quality of life cycle [172]. In this manner, O'Flynn et al. have manufactured a MN-based electrochemical sensor integrated with wireless communication tool for real-time and in-field assessment of soil nitrate levels with minimum energy consumption [144]. MN master mold was fabricated using MEMS technique. After polymer replication, a gold layer was plotted on polymer followed by further copper sputtering to enhance the nitrate conductivity. The nitrate content, which is one of the main components of the fertilizers, was found to be between 15 and 80 μM.

In line with these studies, the health conditions of plant and agricultural products can be continuously monitored for rapid intervention. Moreover, there are innumerable compounds that can be extracted from plants for medical purpose. In addition, MNs are versatile platforms that can be integrated with microflu-

idic platforms, thereby enhancing the separation process of the captured targets using fluid manipulation and surface properties of these microfluidic platforms as demonstrated for diseases [173–175]. Being a rich source for both drug and food production, more studies on MN application as a detection tool in plants need to be extensively continued. MN technology is also applied for disease prevention and treatment [176], which are a turning point for further protection of agricultural products.

Microneedles in prevention and treatment for plant diseases

Precautions for disease-causing substances in plants are crucial. Owing to the detection methods described up to this point, the conditions of healthy and diseased periods of plants can be comprehended, and treatment/prevention processes can be initiated promptly. MNs can deliver agrochemicals or therapeutics in a controlled and easy manner with minimal invasiveness. From this perspective, we here elaborate the utilization and adaptation of MNs in preventing and treating plant disease as shown in timeline (Fig. 1).

One of the most prevalent plant diseases is bacterial infections [177]. *Candidatus Liberibacter asiaticus* (CLas), for instance, causes Huanglongbing (HLB) disease—characterized by citrus greening. Using digital light processing (DLP) 3D printing technology, Santra et al. manufactured coated MNs with a height of 2000 μm and a base radius of 500 μm in delivery of Cu-based therapeutics to the stem tissue of young Valencia orange saplings [22]. Flexible resin-based MN arrays were coated with Cu nanoparticles (NPs) using sodium oleate to create a bind between water in the phloem and the hydrophobic resin. These coated MN arrays have facilitated the penetration to the phloem tissue and transportation of targeted molecules. Continuing the release for 24 h provides slow-release kinetics, thus increasing the killing effect of the platform on HLB-causing bacteria. After this time, the released Cu concentration was measured as approximately 1.5 mg/ml. In conclusion, phytotoxicity-free Cu NPs were transported into the stem part of the saplings to identify and comprehend the transportation control mechanism of therapeutics by enhancing the long-term release potential. Larger amounts of drugs and drug-like molecules can be loaded onto dissolving MNs for release at higher concentrations, and when these MNs degrade in the plant, drugs are released. In addition, with pH responsive and thermoresponsive biopolymers [178,179], delivery can be conducted with an external stimuli.

Agrochemicals such as pesticides and fertilizers have long been used worldwide for the prevention and treatment of plant diseases. Solid MNs can be employed on plants to open pores to further facilitate the transportation of these agrochemicals. Kundu et al. have fabricated MNs with micromilling technique using stainless steel material for the delivery of antimicrobial Zinkicide to the stem of Citrus seedlings (Cleopatra mandarin) (Fig. 10**a**) [18]. The MNs with a base width and height of 500 μm were designed and fabricated to be 19 × 20 arrays and integrated into the paint rollers to facilitate the application on plants in cost- and time-saving manners (Fig. 10**b**). The amount of zinc, which accumulated due to the use of Zinkicide, was monitored to assess the penetration of MN tips and delivery of antimicrobial to the phloem tissues. The process of transporting zinc to the phloem could not be advanced as expected since there was no discernible change in the amount of zinc in the root (Fig. 10**c**). In more detail, approximately 225 μg of Zinc per 1 g of dried plant tissue was measured in the stem part, using MNs, while this amount is approximately 25 μg in the method without the implementation of MN. When three different regions were compared in MN application, the part with the highest release was again measured as 225 μg per 1 g of dried plant tissue in the stem, then approximately 160 μg in the leaf part, and

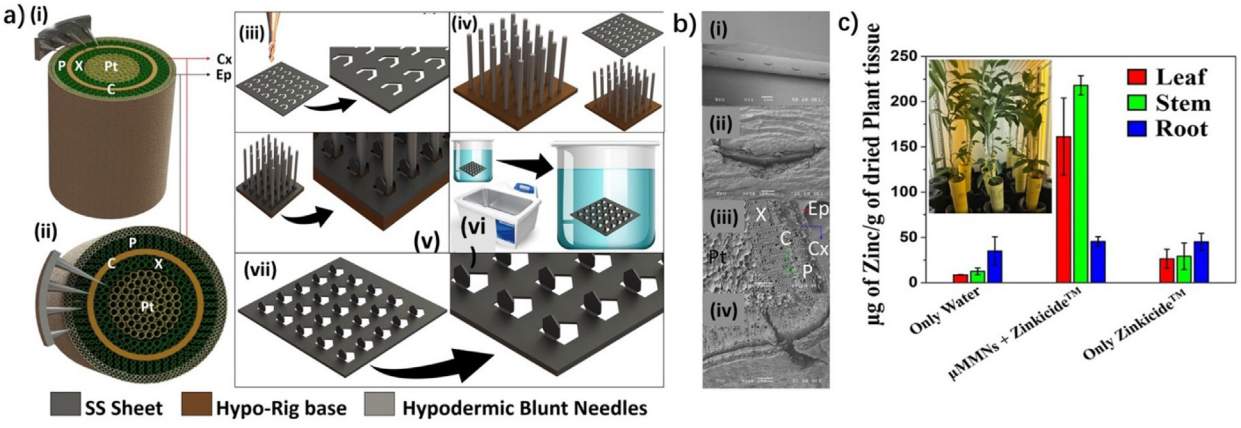

FIG. 10

Micromilled microneedles (μMMNs) were utilized for controlled penetration into plant stem tissue were demonstrated. (a) MN patch penetrated into the different plant parts, and the fabrication process was illustrated. (i) Isometric view of penetrated MN in plant stem tissue. (ii) Top view of penetrated MN in plant stem tissue (iii) Micromilling process utilization to the planar stainless-steel substrate (SS). (iv) Hypo-Rig application for aligning the SS substrate. (v) Transition of μMMNs out of plane. (vi) Removing of debris using acid with sonication. (vii) Final structure of μMMNs. (b) Puncture caused by MNs was imaged using SEM, and amount of Zinc was measured in leaf, stem, and root for three different processes. (i,ii,iii,iv) Punctured stem part of a citrus seedling was monitored using SEM. (c) Zn concentrations are found as approximately 160, 225, and 50 μg per 1 g of dried plant tissue in the leaf, stem, and root after the deployment of therapeutic cargo of ZinkicideTM. The amount of ZinkicideTM observed in the stem without the use of MN was measured as approximately 25 μg per 1 g of dried plant tissue. Reprinted with permission [18]. Copyright 2019, Scientific Reports.

approximately 50 μg in the root where the lowest release was observed. Nonetheless, this technique can still be used to transmit agrochemicals to nearby areas to the phloem region. The length of MN tips and concentration of Zinkicide can be altered to accomplish and improve the required penetration and delivery rates. The use of dissolving MN can increase the efficiency of this release compared to the use of solid MN. These target molecules can be loaded on biocompatible polymers such as gelatin methacryloyl [180], which can be dissolved in water, and the release occurs through degradation. In this way, the possibility of rapid closure of the plant tissue opened with solid MN can be eliminated. On the other hand, smart materials such as thermoresponsive poly(N-isopropylacrylamide) can be utilized for drug delivery with changing its chain structure with the implementation of heat [181].

Another study in which the delivery of agrochemicals to plants with MN technology was conducted by Cao *et al* [176]. Silk-based MNs with a height of 531 ± 39 μm and a base diameter of 226 ± 4 μm were fabricated as cone-shaped and this MN platform was utilized for the release of gibberellic acid (GA3) into *A. thaliana* mutant ft-10 plant. Herein, the wounding time of plant and healing process after this insertion were examined. No matter how low damage MN technology enables, this damage was examined with the observation of healing process. Consequently, post application recovery processes of GA3-loaded MN and non-loaded MN were compared. Healing time of the injured area was boosted three hours after GA3-loaded MN was inserted, whereas this period for the same healing level was 24 h for non-loaded MN. On the other hand, the height of MN decreased substantially down to 148 ± 43 μm (71% decrease rate) after 24 h of application. In addition, the effect of physiological conditions on the growth processes of plants was enhanced by GA3 release. GA3-loaded MN and bare MN were inserted into 7-day rice seedlings and their effect on height growth was investigated. As a result, the GA3-loaded MNs improved physiological processes occurring in the plant. In comparison with the application of agrochemicals by methods such as sprays, the effects of MN-based technology and the significance of the effects pave the way in the field to provide new directions to the researchers, who seek for a vital solution to the delivery challenges in agriculture.

In addition, genome-editing technique has outstanding features for developing nutritional and functional quality of plants. Howbeit, undesirable genetic changes may occur in plants during the delivery of genome-editing protein, and conventional methods may fail to effectively transport the proteins. Viswan et al., for instance, manufactured a MN array with 2 μm width and 60 μm height for delivering genome-editing proteins, i.e., Cre recombinase and Cas9 ribonucleoprotein (RNP), into *A. thaliana* leaves and shoot apical meristem (SAM) in soybean leaves [182]. The MEMS process was utilized for the MNs fabrication. The height of the MN array chips was defined by the initial thickness (2 μm) of the active Si layer, and the photomask was altered to fabricate MN array chips with needles of varying widths (1 and 2 μm) and lengths (40, 60, and 100 μm) on a single wafer. Young's modulus measurement demonstrated that the MN arrays with 2 μm width and 60 μm height were the most efficient in penetrating into the inner layers of these leaf tissues, such as palisade, spongy, and subepidermal L2 layers. The delivery of Cre recombinase into *A. thaliana* was analyzed by the observation of GUS (β-glucuronidase) expression. Furthermore, the PDS11/18 gene in soybean SAM was directly targeted by the Cas9 RNP, which revealed an 11 bp deletion in the target location. The delivery was employed with MN arrays after the drop of these genome-editing proteins in the region of plants. An efficiency of 100% was achieved in all delivery processes. The rate of gene change in the area where the needle was applied was calculated as 6%. This rate was 6.9% in another study [183], demonstrating the efficiency of MN application. Additionally, a mutation rate of only 0.03% was detected. On the other hand, the delivery part of these genome-editing proteins would be enhanced by loading these targets into the dissolving MN types. Moreover, these fluorescence analysis can be analyzed using a machine learning platform to predict further measurements and other crucial probabilities [157].

Besides the enhancements in nutritional and functional attributes of plants using genome-editing proteins, the progresses in the resistance of plants to biotic and abiotic stresses can be accomplished with the delivery of payloads. As an example, Cao et al. have fabricated a MN array using silk fibroin (SF) and α-chymotrypsin (Cs), which provide mechanical strength and solubility features, respectively [184]. The Cs-SF solution (20:80, w:w) was added after mixing with rhodamine 6 g and azoalbumin to PDMS mold and centrifuged before keeping in a fume hood at room temperature overnight. Tobacco and tomato plants were assessed for the analysis of payload delivery and penetration capability of MN arrays without significant deformation. Consequently, fluorescence images exhibited the successful penetration and delivery of MN arrays. After the analysis, 78.7 ng and 38.3 ng of genes could be delivered using xylem and phloem phytoinjector, respectively. This study demonstrated that enhancement in plant health conditions was achieved using payloads of small and large molecules. These stresses can be enhanced by exposing these agrobacterium genes, which are essential in preparing plants for external effects such as bacteria. It has been achieved by this study to produce a better material by utilizing the properties of different biopolymers and to prepare the plant against bacterial infection. The properties of biomaterials used in plant and animal studies, especially with MN, are of great importance in terms of both penetration and release kinetics. In addition to this work, the combination of smart-phone systems, machine learning applications, and autonomous measurement systems can increase the efficiency and in-field usability of future studies [185].

Transient gene expression provides insight in functional proteins of plants [186,187]. Conducting transient expression techniques using particle bombardment and protoplast transformation for agrobacterium infiltration in citrus products is costly and laborious. Acanda et al., for instance, used an affordable, reusable, and reliable method using MN rollers to boost the efficiency [188]. The wounds were first opened on the leaf epidermis using a commercial titanium MNs (DERMAROLL by Prosper Beauty) with a height of 250 μm. Owing to these holes, the agroinfiltration process was facilitated and the expression levels of 100 ng of GFP per milligram was detected. The wound density (70 and 140 wounds/cm^2) and maturity of leaves were found to

impact the expression rate. It was obtained that young leaves provided higher amounts of transient gene expression than old leaves. According to the confocal and western blot results, more GFP-expressing cells were observed around the wounds. The GFP expressing area increased from ~ 10% to ~ 90% in *C. macraphylla* leaves after 6 and 10 days of incubation period, respectively. However, the increase in this area was considerably low for grapefruit and pineapple leaves (from ~ 10% to ~ 30% for grapefruit and ~ 15% to ~ 25% for pineapple leaves). These findings show the positive effect of MNs used on the agroinfiltration process.

Challenges in microneedle in agriculture applications

There are still several challenges that need to be addressed to fully realize MN potential in agricultural products. One of the challenges encountered in MN technology is the fabrication of MN tools which are suitable for use in harsh agricultural environments including hazardous chemicals, high temperatures and humidity, which may easily cause MNs to lose their effectiveness or start degradation before the target analyte is detected or drug is released. Their compatibility with certain substances such as pesticides and fertilizers should be carefully investigated since such substances can be viscous or volatile [189,190].

Plant skin has distinctive features compared to animal skin structure. Plant skin consists of a single layer of cells covering the whole plant surface, this includes leaves, stems, and even roots [191]. These cells possessing cell wall, are tightly packed, which forms a protective layer against water loss, physical damage, pathogens, or UV radiation. These attributes allow plants to have rigid structures. Penetrating into these tissue layers requires the development of MN arrays with high mechanical strength, as well as a unique transport mechanism. This is a critical point as MNs are expected to be fully functional even after multiple application in several agricultural products. The thickness of plant skin layers demonstrates great variation depending on a variety of conditions such as the plant species, its environment, and its stage of growth. Hence, a standardization in MNs for each plant and plant part is needed to expand its use globally.

Agricultural industry is considerably big and require a large number of MNs to be utilized on farms. Hence, the cost of fabrication must be competitive with traditional sensing or delivery methods to make MN technology economically viable. Additionally, significant investment in infrastructure and continuous follow-up of regulatory approval is necessary. The integration of such advanced technologies into agriculture can be slow and MNs may face resistance particularly from farmers and other stakeholders. Although MNs have been largely tested on humans, their adoption by traditional agriculture is still at its infancy. The long-term effects of MNs (particularly dissolving MNs) on environment, soil health, plant growth, yield, and quality must be strictly evaluated to ensure that their use does not have side effects.

Conclusion and future perspectives

Crop diseases in agricultural industry cause yield loss and eventually strike food safety. Over the centuries, agriculture industry has adopted myriads of technological solutions in the pursuit of healthy crops with increased yield. Everlasting belief claiming impracticability of small-scale tools has dominated agricultural habits for years on end. However, recent advances in miniaturized devices designed for treatment, prevention, and detection purpose have already started to threaten current agricultural models. MNs, in this setting, have been a silver lining to the emergence of smart agricultural elaboration.

The use of MNs for such purpose is still in its infancy, and there is a plenty of room at the bottom to exploit such a technological platform. Current agricultural practices of MN-based sensing systems mainly include pathogen detection, metabolite screening, and physiological condition monitoring. Further studies can be also intensified on the detection of the plant species with superior agricultural traits for further reproduction followed by large scale plantation. The researches involving gene delivery to the plants for the treatment of crop diseases and increasing crop resistance against external factors hasn't been explored effectively. To date, only CRISPR-Cas9-mediated genome editing proteins were delivered to *A. thaliana* and soybean leaves via MNs [182]. Transcription activator-like effector nucleases (TALENs) [192] and zinc-finger nucleases (ZFNs) [193] for DNA repair have been gold standards to enhance essential characteristics of agronomic traits. Circular RNAs (circRNAs) as a novel class of endogenous long non-coding RNA can also be a therapeutic agent to manipulate diverse physiological processes in plants [194]. Additionally, small interfering RNA (siRNA) has been a great potential in silencing unwanted genes in plants. The delivery of such genetic machineries to the plants can be significantly enhanced using MN technology.

The effectiveness of MN platforms would be improved by the integration of other systems. Microfluidic platforms can be utilized as emerging systems for the isolation process of these plant pathogens and related metabolites since these platforms are successfully adapted for mammalian cells, proteins, and viruses such as SARS-CoV-2 [195–198]. Moreover, the penetration and sampling capability of MN platforms would enhance the collecting process of target analyte from its native environment, and it can be transferred to the microfluidic platforms. The identification of plant pathogens obtained by MNs would be also improved with technologies such as optical and plasmonic sensors-integrated with microfluidic devices [199–203]. The characterization of numerous pathogens would be possible with the integration of microfluidic platforms with MNs, and the surface properties of both microfluidic devices and MNs would be updated according to the type of target agent. Plant tissues comprise several layers and MNs should be designed accordingly to display minimally-invasive feature during sampling or delivery of therapeutics. Artificial intelligence frameworks can be developed to assess and predict optimum features of MNs including size, number, type, and material to design specific platform(s) to each plant type and part [204]. Furthermore, machine learning-assisted optimization can be introduced to accelerate the design process of MNs, by this means, reducing the overall cost.

Smart materials exhibit high sensitivity to the alterations in an external stimulus. Due to their unique chemical and physical features, they have far-reaching potential in MN fabrication [205]. Materials such as silk are charming biomaterials with

excellent hierarchical structures and outstanding characteristics. Novel biopolymers with distinct stimuli-responsive properties (e.g., pH-responsive, temperature-responsive, light-responsive, and redox-responsive etc.) can be designed to detect or deliver agricultural elements in an intelligent fashion, through this way, eliminating uncontrolled administration of drugs such as pesticides. Additional integration of wireless technologies with MNs can enable real-time monitoring and further facilitate in-field implementation of MNs.

Data availability

Data will be made available on request.

Declaration of Competing Interest

The authors declare that they have no known competing financial interests or personal relationships that could have appeared to influence the work reported in this paper.

Acknowledgement

Fatih Inci gratefully acknowledges support from the Scientific and Technological Research Council of Turkey (TÜBİTAK) 2232 International Fellowship for Outstanding Researchers (Project No: 118C254) and the Turkish Academy of Sciences Outstanding Young Scientists Award Program (TÜBA-GEBİP). Ismail Eş also thanks the support from TÜBİTAK 2232 Project (Project No: 118C254). However, the entire responsibility of the publication/article belongs to the owner of the publication/article. The financial support received from TÜBİTAK does not mean that the content of the publication is approved in a scientific sense by TÜBİTAK. Emre Ece and Fatih Inci also thank the TÜBİTAK 1001 Scientific and Technological Research Projects Funding Program (Project No: 120Z445) for support. This work was also supported by the Young Scientist Awards Program (BAGEP) award from the Science Academy.

References

[1] United Nations Department of Economic and Social Affairs, Global Population Growth and Sustainable Development, 2021.
[2] U. Jumhawan, T. Bamba, in: Appl. Green Solvents Sep. Process., Elsevier, 2017, pp. 483–516.
[3] M. Eskola et al., Crit. Rev. Food Sci. Nutr. 60 (2020) 2773–2789.
[4] T.N. Liliane, M.S. Charles, Agron. Chang. Food Secur. (2020) 9.
[5] T. Swaroopa Rani et al., in: Agrochem. Detect. Treat. Remediat., Butterworth-Heinemann, 2020, pp. 437–464.
[6] A. Alengebawy et al., Toxics 9 (2021) 42.
[7] V.L. Zikankuba et al., Cogent Food Agric. 5 (2019) 1601544.
[8] H. Senyuva, in: Encycl. Food Saf., Academic Press, Waltham, 2014, pp. 152–158.
[9] N. Kaur et al., Curr. Opin. Green Sustain. Chem. 30 (2021) 100488.
[10] Y. Ji et al., Mater. Interfaces 13 (2021) 43374–43386.
[11] C. An et al., J. Nanobiotechnology 20 (2022) 1–19.
[12] D. Kaushik et al., in: Handb. Non-Invasive Drug Deliv. Syst., William Andrew Publishing, Boston, 2010, pp. 135–164.
[13] W. Shu et al., Acta Biomater. 135 (2021) 403–413.
[14] Ö. Erdem et al., Biosensors 11 (2021) 296.
[15] X. Hong et al., Nano-Micro Lett. 6 (2014) 191–199.
[16] K.J. Krieger et al., Microsystems Nanoeng. 5 (2019) 1–14.
[17] Y. Li et al., Microsystems Nanoeng. 5 (2019) 1–11.
[18] A. Kundu, M.G. Nogueira Campos, S. Santra, S. Rajaraman, Sci. Rep. 9 (2019) 1–8.
[19] H.X. Nguyen, A.K. Banga, Pharm. Res. 35 (2018) 1–20.
[20] P. Dardano, I. Rea, L. De Stefano, Curr. Opin. Electrochem. 17 (2019) 121–127.
[21] R. Liu, X.H. Wang, F. Tang, Y.Y. Feng, Z.Y. Zhou, in: 13th Int. Conf. Solid-State Sensors, Actuators Microsystems, 2005. Dig. Tech. Pap. TRANSDUCERS'05., IEEE, 2005, pp. 1517–1520.
[22] L. Santra et al., IEEE 34th Int. Conf. Micro Electro Mech. Syst. IEEE 2021 (2021) 630–633.
[23] G. Du et al., J. Control. Release 336 (2021) 537–548.
[24] R. Paul et al., ACS Nano 13 (2019) 6540–6549.
[25] S.M. Mugo, W. Lu, Anal. Bioanal. Chem. 412 (2020) 7063–7072.
[26] S. Baek et al., J. Microelectromechanical Syst. 27 (2018) 440–447.
[27] Z. Wang et al., Mater. Sci. Eng. C 127 (2021) 112237.
[28] N.I. Hossain, S. Tabassum, IEEE 17th Int. Conf. Nano/Micro Eng. Mol. Syst. IEEE 2022 (2022) 312–316.
[29] E. Jeon et al., J. Micromechanics Microengineering 27 (2017) 85009.
[30] Z. Faraji Rad, Adv. Eng. Mater. 25 (2023) 2201194.
[31] C.K. Maisels, The Emergence of Civilization: From Hunting and Gathering to Agriculture, Cities, and the State of the near East, Routledge, 2003.
[32] J.L. Araus et al., J. Exp. Bot. 58 (2007) 131–145.
[33] Food and Agriculture Organization, (2020). (access date: 10.22.2022).
[34] STEPHEN D. SIMPSON, Investopedia (2021).
[35] L.K. Johnson et al., Resour. Conserv. Recycl. 137 (2018) 243–250.
[36] Food and Agriculture Organization of the United Nations, Climate Change Fans Spread of Pests and Threatens Plants and Crops, New FAO Study, 2019.
[37] M.W. Kujawski, J. Namieśnik, TrAC Trends Anal. Chem. 27 (2008) 785–793.
[38] F. Ahmad, O.O. Babalola, H.I. Tak, Anal. Bioanal. Chem. 404 (2012) 1247–1255.
[39] A.-K. Mahlein, Plant Dis. 100 (2016) 241–251.
[40] F.B. Iriarte et al., Bacteriophage 2 (2012) e23530.
[41] M. Khater, A. De La Escosura-Muñiz, A. Merkoçi, Biosens. Bioelectron. 93 (2017) 72–86.
[42] H.Y. Lau, J.R. Botella, Front. Plant Sci. 8 (2017).
[43] X. Huang et al., Analyst 143 (2018) 5339–5351.
[44] A.H. Cobb, J.P.H. Reade, Herbicides and Plant Physiology, Wiley-Blackwell, Oxford, UK, 2010.
[45] H.F. Kraybill, Insecticides, Action and Metabolism, 1968.
[46] C.E. Yarwood, Science (80-.) 103 (1946) 87.
[47] G. Matthews, R. Bateman, P. Miller, Pesticide Application Methods, John Wiley & Sons, 2014.
[48] R.J. Feldmann, H.I. Maibach, Toxicol. Appl. Pharmacol. 28 (1974) 126–132.
[49] F. Inci et al., Forensic Sci. Int. Genet. 52 (2021) 102451.
[50] S. Deshmukh et al., Forensic Sci. Int. Genet. 48 (2020) 102313.
[51] F. Inci et al., Appl. Mater. Today 18 (2020) 100478.
[52] A. Mataji-Kojouri et al., ACS Nano 14 (2020) 8518–8527.
[53] F. Inci et al., Appl. Mater. Today 20 (2020) 100709.
[54] F. Inci et al., Proc. Natl. Acad. Sci. 112 (2015).
[55] F. Inci et al., Biochem. Biophys. Reports 2 (2015) 115–122.
[56] L. Luan et al., J. 8 (2008) 628–635.
[57] H. Shafiee et al., Sci. Rep. 5 (2015) 8719.
[58] S. Julich et al., Biosens. Bioelectron. 26 (2011) 4070–4075.
[59] F. Inci et al., Adv. Sci. 5 (2018) 1800121.
[60] J. Tomlinson, C.A.B. Rev, Perspect. Agric. Vet. Sci. Nutr. Nat. Resour. 3 (2008).
[61] A.M. D'Onghia et al., J. Plant Pathol. 83 (2001) 139–142.
[62] R. Paul et al., Curr. Protoc. Plant Biol. 5 (2020).
[63] M. Pumera, A. Merkoçi, S. Alegret, TrAC Trends Anal. Chem. 25 (2006) 219–235.
[64] Y. Huang, A.J. Mason, Lab Chip 13 (2013) 3929.
[65] M. Yucel et al., Anal. Chem. 90 (2018) 5122–5129.
[66] M.S. Gerstel, V.A. Place, (1976).
[67] D. V McAllister, S. Henry, M.G. Allen, M.R. Prausnitz, in: Proc. Control. Release Soc., Elsevier, 1998, pp. 30–31.
[68] Y. Li et al., Eur. J. Pharm. Sci. 151 (2020) 105361.
[69] S.P. Sullivan, N. Murthy, M.R. Prausnitz, Adv. Mater. 20 (2008) 933–938.
[70] J. Ji, F.E.H. Tay, J. Miao, J. Phys. Conf. Ser. 34 (2006) 1132–1136.
[71] P. Makvandi et al., Nano-Micro Lett. 13 (2021) 93.
[72] R.R. Thakur Singh et al., Expert Opin. Drug Deliv. 14 (2017) 525–537.
[73] A.M. Römgens et al., Comput. Methods Biomech. Biomed. Engin. 19 (2016) 1599–1609.
[74] S. Dugam et al., Futur J. Pharm. Sci. 7 (2021) 19.
[75] P. Aggarwal, C.R. Johnston, Sensors Actuators B Chem. 102 (2004) 226–234.
[76] J. de Wit et al., Appl. Opt. 59 (2020) 10304–10311.
[77] K. Nair et al., Pharmaceutics 7 (2015) 471–485.
[78] W. Li et al., J. Control. Release 347 (2022) 489–499.
[79] K.T.M. Tran et al., Nat. Biomed. Eng. 5 (2020) 998–1007.
[80] S. Pahal et al., Eur. J. Pharm. Biopharm. 159 (2021) 151–169.
[81] A. Davidson, B. Al-Qallaf, D.B. Das, Chem. Eng. Res. Des. 86 (2008) 1196–1206.

[82] S.N. Economidou, D. Douroumis, Adv. Drug Deliv. Rev. 173 (2021) 60–69.
[83] M.R. Prausnitz, Adv. Drug Deliv. Rev. 56 (2004) 581–587.
[84] H.R. Nejad et al., Microsystems Nanoeng. 4 (2018) 1–7.
[85] M. Tilli et al., Handbook of Silicon Based MEMS Materials and Technologies, Elsevier, 2020.
[86] E.R. Parker et al., J. Microelectromechanical Syst. 16 (2007) 289–295.
[87] K. Yoshida et al., Med. Biol. Eng. Comput. 45 (2007) 413–420.
[88] M. Hoang, K. Ita, D. Bair, Pharmaceutics 7 (2015) 379–396.
[89] J.G. Turner et al., Macromol. Biosci. 21 (2021) 2000307.
[90] S.-O. Choi et al., Biomed. Microdevices 12 (2010) 263–273.
[91] Y. Hao et al., J. Biomed. Nanotechnol. 13 (2017) 1581–1597.
[92] M. Wang, L. Hu, C. Xu, Lab Chip 17 (2017) 1373–1387.
[93] X. He et al., Dose-Response 17 (2019) 1559325819878585.
[94] Q.L. Wang et al., Mater. Sci. Eng. C 65 (2016) 135–142.
[95] A. Sadeqi et al., 40th Annu. Int. Conf. IEEE Eng. Med. Biol. Soc. IEEE 2018 (2018) 5737–5740.
[96] D.-S. Kim et al., Pharm. Res. 37 (2020) 50.
[97] K.J. Cha et al., J. Micromechanics Microengineering 24 (2014) 115015.
[98] N. Dragicevic, H.I. Maibach, Percutaneous Penetration Enhancers Physical Methods in Penetration Enhancement, Springer, 2017.
[99] M. Gülçür et al., J. Manuf. Sci. Technol. 32 (2021) 311–321.
[100] J. Li et al., Mater. Sci. Eng. C 96 (2019) 576–582.
[101] P.R. Miller et al., MRS Adv. 4 (2019) 1417–1426.
[102] K. Lee et al., Adv. Mater. 22 (2010) 483–486.
[103] M.J. Kim et al., Front. Bioeng. Biotechnol. 6 (2018) 54.
[104] Z. FarajiRad, P.D. Prewett, G.J. Davies, Microsystems Nanoeng. 7 (2021) 71.
[105] G. Yan et al., Int. J. Pharm. 391 (2010) 7–12.
[106] Q.Y. Li et al., Rsc Adv. 7 (2017) 15408–15415.
[107] K.J. Lee et al., Int. J. Pharm. 573 (2020) 118778.
[108] K. Park, J. Control. Release Off. J. Control. Release Soc. 120 (2007) 1.
[109] K. Ita, J. Drug Deliv. Sci. Technol. 44 (2018) 314–322.
[110] H.J.G.E. Gardeniers et al., J. Microelectromechanical Syst. 12 (2003) 855–862.
[111] B. Ahn, Int. J. Control. Autom. Syst. 18 (2020) 143–149.
[112] S.P. Davis, M.R. Prausnitz, M.G. Allen, in: TRANSDUCERS '03. 12th Int. Conf. Solid-State Sensors, Actuators Microsystems. Dig. Tech. Pap. (Cat. No.03TH8664), IEEE, n.d., pp. 1435–1438.
[113] P. Dardano et al., Polymers (Basel). 13 (2021) 520.
[114] J. Jiang et al., Pharm. Res. 26 (2009) 395–403.
[115] S.H. Bariya et al., J. Pharm. Pharmacol. 64 (2012) 11–29.
[116] M. Suzuki, T. Takahashi, S. Aoyagi, Int. J. Nanotechnol. 15 (2018) 157–173.
[117] H. Kim, S.K. Moon, M. Seo, Microelectron. Eng. 153 (2016) 15–19.
[118] H. Le Thanh et al., J. Microelectromechanical Syst. 24 (2015) 1583–1593.
[119] M.W. Zhu et al., J. Micromechanics Microengineering 19 (2009) 115010.
[120] J.C. Harper et al., Mater. Interfaces 1 (2009) 1591–1598.
[121] R. Nagarkar et al., J. Drug Deliv. Sci. Technol. 59 (2020) 101923.
[122] K. Ita, Biomed. Pharmacother. 93 (2017) 1116–1127.
[123] X. Jin et al., Adv. Drug Deliv. Rev. 127 (2018) 119–137.
[124] S. Lin et al., Eur. J. Pharm. Biopharm. 122 (2018) 104–112.
[125] S.H. Lim et al., J. Control. Release 329 (2021) 907–918.
[126] A.M. Rodgers, A.J. Courtenay, R.F. Donnelly, Expert Opin. Drug Deliv. 15 (2018) 1039–1043.
[127] K. Lee, H. Jung, Biomaterials 33 (2012) 7309–7326.
[128] J. Li et al., Curr. Med. Chem. 24 (2017) 2413–2422.
[129] L.K. Vora et al., Int. J. Biol. Macromol. 146 (2020) 290–298.
[130] S. Amodwala, P. Kumar, H.P. Thakkar, Eur. J. Pharm. Sci. 104 (2017) 114–123.
[131] S. Sharma et al., Anal. Methods 10 (2018) 2088–2095.
[132] B. Al-Qallaf, D.B. Das, A. Davidson, Asia-Pacific J. Chem. Eng. 4 (2009) 845–857.
[133] A.K. Andrianov, A. Marin, D.P. DeCollibus, Pharm. Res. 28 (2011) 58–65.
[134] R. Haj-Ahmad et al., Pharmaceutics 7 (2015) 486–502.
[135] R.S.J. Ingrole, H.S. Gill, J. Pharmacol. Exp. Ther. 370 (2019) 555–569.
[136] H.S. Gill, M.R. Prausnitz, J. Control. Release 117 (2007) 227–237.
[137] Y. Zhang et al., Pharm. Res. 29 (2012) 170–177.
[138] M.J. Uddin et al., Int. J. Pharm. 494 (2015) 593–602.
[139] J.A. Matriano et al., Pharm. Res. 19 (2002) 63–70.
[140] X. Chen et al., J. Control. Release 139 (2009) 212–220.
[141] M.G. McGrath et al., Int. J. Pharm. 415 (2011) 140–149.
[142] C.E. Chandler et al., Infect. Immun. 86 (2018) e00406–e00418.
[143] A. Bukhamsin et al., Adv. Sci. 8 (2021) 2101261.
[144] B. O'Flynn et al., IEEE SENSORS, IEEE 2017 (2017) 1–3.
[145] J.-H. Park et al., Eur. J. Pharm. Biopharm. 76 (2010) 282–289.
[146] S.A. Coulman et al., Int. J. Pharm. 366 (2009) 190–200.
[147] L.Y. Chu, S.-O. Choi, M.R. Prausnitz, J. Pharm. Sci. 99 (2010) 4228–4238.
[148] A.M.V. Mohan et al., Biosens. Bioelectron. 91 (2017) 574–579.
[149] J.R. Windmiller et al., Electroanalysis 23 (2011) 2302–2309.
[150] B. Ciui et al., Adv. Healthc. Mater. 7 (2018) 1701264.
[151] S. Kawakami, Y. Watanabe, R.N. Beachy, Proc. Natl. Acad. Sci. 101 (2004) 6291–6296.
[152] B. Moury et al., Phytopathology 91 (2001) 84–91.
[153] R.P. Singh et al., Plant Dis. 90 (2006) 1457.
[154] J. Penney et al., J. Med. Virol. 94 (2022) 3978–3981.
[155] D. Khodakov et al., Nat. Biomed. Eng. 5 (2021) 702–712.
[156] R. Paul et al., Biosens. Bioelectron. 187 (2021) 113312.
[157] H. Ceylan Koydemir et al., Nanophotonics 6 (2017) 731–741.
[158] W. Batista-Silva et al., Front. Plant Sci. 9 (2018) 1689.
[159] M. Efenberger-Szmechtyk, A. Nowak, A. Czyzowska, Crit. Rev. Food Sci. Nutr. 61 (2021) 149–178.
[160] X. Dong, M.C. Vuran, S. Irmak, Ad Hoc Networks 11 (2013) 1975–1987.
[161] L.M. Srivastava, in: Plant Growth Dev., Elsevier, 2002, pp. 217–232.
[162] E. Nambara, in: Encycl. Appl. Plant Sci., Elsevier, 2017, pp. 361–366.
[163] Y. Lu et al., Nano Energy 58 (2019) 624–632.
[164] C. Hegarty et al., Mater. Chem. Phys. 227 (2019) 340–346.
[165] H. Yin et al., Adv. Mater. 33 (2021) 2007764.
[166] M.E.H. Chowdhury et al., Sensors 20 (2020) 5637.
[167] R. Branco et al., Protoplasma 254 (2017) 1127–1137.
[168] A. Bukhamsin et al., IEEE 33rd Int. Conf. Micro Electro Mech. Syst. IEEE 2020 (2020) 307–310.
[169] L.J. Gordon, C.M. Finlayson, M. Falkenmark, Agric. Water Manag. 97 (2010) 512–519.
[170] S.-H. Cai et al., Int. J. Mass Spectrom. 473 (2022) 116793.
[171] U.W. Liebal et al., Metabolites 10 (2020) 243.
[172] U. De Corato, Sci. Total Environ. 738 (2020) 139840.
[173] S.Z. Shirejini, F. Inci, Biotechnol. Adv. 54 (2022) 107814.
[174] G.A. Akceoglu, Y. Saylan, F. Inci, Adv. Mater. Technol. 6 (2021) 2100049.
[175] S. Wang et al., Int. J. Nanomedicine 7 (2012) 2591–2600.
[176] Y. Cao et al., Adv. Mater. (2022) 2205794.
[177] S.G. Borkar, R.A. Yumlembam, Bacterial Diseases of Crop Plants, CRC Press, 2016.
[178] K.A. Soliman et al., Drug Discov. Today 24 (2019) 1575–1586.
[179] C. Qian et al., Int. J. Biol. Macromol. 123 (2019) 140–148.
[180] Z. Luo et al., Adv. Healthc. Mater. 8 (2019) 1801054.
[181] D. Coughlan, O. Corrigan, Int. J. Pharm. 313 (2006) 163–174.
[182] A. Viswan et al., Front. Plant Sci. 13 (2022).
[183] Y. Liu et al., Front. Plant Sci. 12 (2021).
[184] Y. Cao et al., Adv. Sci. 7 (2020) 1903551.
[185] J.-H. Kim et al., BioChip J. 9 (2015) 285–292.
[186] S. Ueki, S. Magori, B. Lacroix, V. Citovsky, in: Biolistic DNA Deliv., Humana Press, Totowa, NJ, 2013, pp. 17–26.
[187] D. Cai, N. Kaul, T.A. Lionberger, D.M. Wiener, K.J. Verhey, E. Meyhofer, in: 2010, pp. 81–107.
[188] Y. Acanda et al., Plant Cell Rep. 40 (2021) 1171–1179.
[189] M.L. Alonso et al., J. Chem. Technol. Biotechnol. 89 (2014) 1077–1085.
[190] T. Kromer et al., Environ. Sci. Pollut. Res. 11 (2004) 107–120.
[191] M. Javelle et al., New Phytol. 189 (2011) 17–39.
[192] Y. Wang et al., J. Qiu 32 (2014) 947–952.
[193] F.D. Urnov et al., Nat. Rev. Genet. 11 (2010) 636–646.
[194] L. Santer, C. Bär, T. Thum, Mol. Ther. 27 (2019) 1350–1363.
[195] K. Sagdic, F. Inci, Adv. Eng. Mater. 24 (2022) 2100857.
[196] F. Inci, Langmuir 38 (2022) 1897–1909.
[197] Ö. Erdem et al., Anal. Chem. 94 (2022) 3–25.
[198] E. Derin, F. Inci, ACS Sensors 7 (2022) 358–385.
[199] G. Xing et al., Chinese Chem. Lett. 33 (2022) 1743–1751.
[200] F. Inci et al., ACS Nano 7 (2013) 4733–4745.
[201] B. Kuswandi, Nuriman, J. Huskens, W. Verboom, Anal. Chim. Acta 601 (2007) 141–155.
[202] Ö. Erdem et al., Emergent Mater. 4 (2021) 169–185.
[203] F. Incï, Hacettepe J. Biol. Chem. (2022).
[204] M. Rezapour Sarabi et al., Biosensors 12 (2022) 491.
[205] K. Sagdic et al., Trends Biotechnol. (2022).
[206] J. Hendrichs, R. Pereira, M.J.B. Vreysen, Area-Wide Integrated Pest Management, CRC Press, Boca Raton, 2021.
[207] Charles Onians, (2019). (access date: 04.10.2022).
[208] M.A. Dita, L.P. Vicente, E. Martínez, Food Agric. Organ. United Nations. Tech. Man. (2014) 1–75.
[209] E. Strobl, P. Mohan, Atmosphere (Basel). 11 (2020) 947.
[210] S. McCook, J. Vandermeer, Phytopathology® 105 (2015) 1164–1173.

[211] A. Abbas, T. Yli-Mattila, Toxins (Basel). 14 (2022) 299.
[212] A.Y. Bandara et al., PLoS One 15 (2020) e0231141.
[213] Y. Tian et al., J. Pharm. Sci. 111 (2022) 1070–1080.
[214] Y. Shin et al., Sci. Rep. 12 (2022) 12189.
[215] H. Pitakjakpipop et al., Biomacromolecules 23 (2022) 365–376.
[216] C.K. Choi et al., Eur. J. Pharm. Biopharm. 83 (2013) 224–233.
[217] R. Vecchione et al., Adv. Funct. Mater. 24 (2014) 3515–3523.
[218] S. Mckee et al., J. Photochem. Photobiol. B Biol. 229 (2022) 112424.
[219] O. Howells et al., Eur. J. Pharm. Biopharm. 171 (2022) 19–28.
[220] A. Al Mamun et al., Sensors Actuators A Phys. 336 (2022) 113407.